Manufacturing of Microcapsules With Liquid Core and Their Self-Healing Performance In Epoxy for Resin Transfer Moulding

by

Çağatay Yılmaz

Submitted to
the Graduate School of Engineering and Natural Sciences
in partial requirements for the degree of
Master of Science

SABANCI UNIVERSITY

August 2013

APPROVED BY:

Mehmet Yıldız .....

(Thesis Supervisor)

Yusuf Menceloğlu .....

(Co-advisor)

Bahattin Koç .....

Özge Akbulut .....

Alpay Taralp .....

DATE OF APPROVAL: .....

"The mystery of life is not a problem to be solved but a reality to be experienced.."

Art Van Der Leeuw

Manufacturing of Microcapsules With Liquid Core and Their Self-Healing Performance In Epoxy for Resin Transfer Moulding

Çağatay Yılmaz

Mat, M.Sc. Thesis, 2013

Thesis Supervisor: Assoc. Prof. Dr. Mehmet Yıldız

Keywords: self-healing, microcapsules, in-situ polymerization, RTM-epoxy resin

Abstract

Microcapsules with different active core materials have been receiving a great deal of attention for developing polymer based materials with selfhealing abilities. The self-healing ability is crucial in particular for matrix materials having brittle nature such as epoxy resin. In order for abstaining from an abrupt failure of structural brittle manner polymeric materials, microcapsules can be used excellently as a viable repair agent. In this work, we present a study on the catalyst-free microcapsule based self-healing system. Microcapsules were produced by the in-situ polymerization of urea-formaldehyde at the dispersed phase-water interface. Each microcapsule batches were characterized by using Fourier Transform Infrared Spectroscopy (FTIR), Thermogravimetric Analyser (TGA), Differential Scanning Calorimetry (DSC). Characteristic peaks of urea-formaldehyde shell, core components; DGEBA, and PhCl was seen in the Mid- IR region. Characteristic thermal decomposition temperature of urea-formaldehyde wall material and DBEBA which is the main microcapsule content were determined from the TGA trace. In addition to the given thermal and spectral characterization tools, optic microscope and SEM images also ensure the formation of liquid-filled microcapsules. Although the microcapsules showed brittle behavior during the processing such as drying and sieving, incorporation of microcapsules into the epoxy matrix was achieved successfully. The healing characteristic of epoxy-microcapsule composite was assessed by the Tapered Double Cantilever Beam (TDCB) specimen at the mode-I crack opening fashion. Besides microcapsule-epoxy composite system showed a moderate healing efficiency, a significant increase in mode-I fracture toughness value was observed. Three point bending experiment was also conducted on the microcapsule-epoxy composite. It was found that microcapsules drastically decrease the flexure strength of questioned host material.

Sıvı Çekirdek İçeren Mikrokapsülerin Üretimi ve Bu Kapsüllerin Reçine Transfer Kalıplama Yönteminde Kullanılan Epoksi Reçine İçinde Onarım Performansları

Çağatay Yılmaz

Mat, M.Sc. Tez, 2013

Tez Danışmanı: Doç. Dr. Mehmet Yıldız

Anahtar Kelimeler: kendini onarabilme, mikrokapsül, in-situ polimerizasyonu, epoksi

Özet

Farklı reaktif kor materyallari içeren mikrokapsüllere dayalı polimer tabanlı kendini onarabilme sistemleri son zamanlarda büyük dikkat çekmektedir. Kendini onarabilme yeteneği, epoksi gibi kırılgan yapıya sahip polimerler için çok önem arzetmektedir. Kırılgan yapıya sahip polimerik malzemelerin beklenmedik bir anda servis dışı kalmasını engellemek için onarım solüsyonu içeren mikrokapsüller kullanılabilir. Bu tezin içeriğinde tekli mikrokapsül sistemine sahip taban malzemenin kendini onarabilme yeteneği üzerine bir çalışma sunulmaktadır. Mikrokapsüller dağıtılmış faz-ana faz yüzeyinde gerçekleşen üre-formaldehit in-situ polimerizasyonu ile üretil-mişlerdir. Her bir mikrokapsül banyosu Fourier Dönüşümlü Kızılötesi Spektroskopisi (FTIR), Termogravimetrik Analiz (TGA), ve Diferansiyel Taramalı Kalorimetri (DSC) kullanılarak karakterize edilmiştir. Mikrokapsüllerin kabuklarına ve onarım solüsyonuna ait spektral karakteristik pikler orta-kızılötesi bölgede analiz edilmiştir. Ure-formaldehit duvar malzemesine ve ana mikro kapsül bileşeni olan DGEBA' ya ait termal bozulma sıcaklıkları analiz edilmiştir. Bunlara ek olarak Optik mikroskop ve SEM fotografları da sıvı onarım ajanı dolu mikrokapsüllerin oluşumunu teyit etmiştir. Sıvı onarım ajanı içeren kapsüller üretim aşamasında kırılgan bir davranış sergilemiş olsa da taban materyale başarıyla eklenmiştir. Seçilen taban malzemenin kendini onarabilme verimi ve özelliği incelen çift dirsekli kiriş (İÇDK) ile mode-I çatlak açılması yöntemi kullanılarak incelenmiştir. Mikrokapsul-epoksi kompozit sistemi düşük onarım verimlilikleri göstermesine rağmen, aynı sistemin mode-I kırılma tokluğu değerinde kayde değer artış gözlenmiştir. Üç nokta bükülme deneyi ayrıca mikrokapsül-epoksi kompozitin bükülme mukavemeti değerini ölçmek için yapılmış ve sonuçta mikrokapsüllü örneklerin bükülme mukavemetlerin de ciddi oranlar da düşüşler gözlenmiştir.

Acknowledgements

I would like to thank to **Professor Mehmet Yıldız** and **Professor Yusuf Menceloğlu** as my advisor.

My reading committee members, Professors **Bahattin Koç**, **Özge Akbulut**, **Alpay Taralp**, for their helpful comments on the draft of this thesis.

Sabanci University Academic Support Program for funding my graduate education for two years

My colleagues at our laboratory, Fazlı Fatih Melemez, Dr. Pandian Chelliah, Ataman Deniz, Esat Selim Kocaman, and Talha Boz for their friendship, helps and guidance during the course of my thesis.

My friends at Sabanci University Rıdvan Demiryürek, Serkan Yalıman, Furkan Aytuğan, Dilek Çakıroğlu, Kinyas Aydın, İlker Kalyoncu, Mariamu Kassim Ali, Erim Ülkümen, Senem Avaz, Melike Mercan Yildizhan, Mustafa Baysal, Aslihan Örüm, Güliz İnan, Tuğçe Akkaş, Ezgi Dündar Tekkaya, Amin Rahmat, Amin Yaghoobi, Mohammadreza Khodabakhsh, Mustafa Yalçın

My brother Furkan Yılmaz

My family for their unending sport from the beginning of my life.

To all of you, Thank you!

Çağatay Yılmaz

Contents

List of Figures

List of Tables

Abbreviations

TDCB	**T**apered **D**ouble **C**antilever **B**eam
DCB	**D**ouble **C**antilever **B**eam
STA	**S**imultaneous **T**hermal **A**nalsis
TGA	**T**hermal **G**ravimetric **A**nalysis
DSC	**D**ifferential **S**canning **C**alorimetry
FTIR	**F**ourier **T**ransform **I**nfrared **S**pectroscopy
ATR	**A**ttenuated **T**otal **R**eflectance
SEM	**S**canning **E**lectron **M**icroscopy
UTM	**U**niversal **T**esting **M**achine
DGEBA	**D**iglycidyl **E**ther of **B**isphenol-A
PhCl	**C**hlorobenzene
EMA	**E**thylene **M**aleic **A**nhyride Copolymer

Physical Constants

TDCB Stress Intensity Geometric Constant	α	=	$11.2 \times 10^3\ m^{-3/2}$
Viscosity of DGEBA	η	=	$0.78\ Pas$
Viscosity of PhCl	η	=	$0.75 \times 10^{-3}\ Pas$
Dielectric constant of PhCl	ϵ	=	5.7
Dielectric constant of Water	ϵ	=	80

Symbols

G	strain energy	Jm^{-2}
P	load	N
h	specimen height profile	mm
b	specimen thickness	mm
E	energy in system	J
W	work done by the system	J
δ	cross head displacement	μm
K	kinetic energy in system	J
da/dN	fatigue crack growth rate	mm/cycle
a	crack length	mm
A	total crack area	mm^2
b_n	thickness in the crack plane	mm
C	compliance	mm/N
u	displacement	mm
ε_{xx}	normal strain in x-direction	
ε_{xy}	shear strain in x-y plane	
M	bending moment	Nm
E	young modulus	GPa
I	moment of inertia of a plane area	m^4
ν	Poisson's ratio	
Q	shear force	N
σ_{yy}	normal stress in y-direction	MPa
σ_{xy}	shear stress in x-y plane	MPa

K_{IC}	mode-I fracture toughness	$\mathrm{MPam}^{1/2}$
m	TDCB geometric constant	mm^{-1}

To my grandmother Sultan and my grandfather Kahraman. . .

Chapter 1

Introduction

1.1 Motivation

Degradation, damage, and eventually failure occur to all human-made materials [3]. Moreover all engineered materials ultimately fail because of environmental or mechanical reasons. There is only one way to provide reliability of the entire structure. Structures are taken out of service for periodic inspection in order to ensure reliability of the material [4]. If there is any uncertainty in any part of the structure, that part has to be replaced with a new one. This process is time consuming and increases the operating cost of the structure. Moreover, inspection of the entire structure needs some external test machines and labor. Sometimes, the whole structure may need to be disassembled in order to check certain parts, as is the case for airplanes, ships and spacecrafts. After splintering and testing the parts, the reassembly of the parts can cause unpredicted challenges.

On the other hand, living organisms handle the unwanted damage with an old-fashioned approach: namely, by self-healing. This approach may have been used since the first living organism existed on the earth. Today, engineers and scientist search for the adaptation of this self healing approach to structural material.

Incorporation of a smart functionality into the engineering material can both provide a reliable and cost effective material system. According to 2013 NACE study, total cost of corrosion to USA economy will exceed $1 trillion. A self healing

corrosion coating might diminish this huge value and provide a sustainable metal structure over the years.

Whenever self-healing is called for engineering material, it is assumed that materials mend themselves to repair defects. This phenomena seems far-fetched because firstly material must recognize damage, this can be only achieved by the incorporation of sensors into the structure then by the aid of external hardware and software, healing mechanism can be triggered to make a decision whether or not to transport healing material to the damaged area. This process also requires external energy and highly engineered sensors. Therefore this idea can be very costly and ineffective for applications that need lightweight material. The external energy supply and hardware can make the system heavier. If it is necessary to establish a reasonable self-healing material, we must turn our attention to living organisms. It must be understood exactly what they do to repair their damage. For example, we can investigate human skin. What it does when scratched and how it achieves repairing the scar; we can even follow plants to learn their self-repair process as well. If we consider human skin when it get damaged, firstly an inflammatory response (immediately, blood clotting) occurs, secondly cell proliferation starts, finally matrix remodeling happens. Today, the most promising artificial self-healing approach based on this model: by microcapsule based self-healing materials. When cracks occur in structural material, it needs a triggering mechanism to activate the healing process. Microcapsule based self-healing materials use almost the same methodology as the human skin. There are three steps in this approach: actuation, transport and chemical repair. Actuation causes the transport of the healing agent to the damaged area. Transport initiates chemical repairing on the damaged part.

To achieve a reasonable self-healing material, it is necessary to study mechanical properties and the damage mode of the host material of interest. It must be understood what kind of damage modes occur in the host material during its service life, since it is almost impossible to repair all damage modes with an artificial self-healing approach. An optimum self healing system should both provide a self healing ability to the host material and do not cause to decrease any mechanical properties of the sample of interest. Delamination, fiber debonding, indentation, surface cracking, transverse and shear cracking, cut in coating and corrosion in metal substrate, scratch and micro cracking are the main damage types in polymer, composites, metal and metal coatings. Todays self-healing approach has

focused on the polymer, glass fiber or carbon fiber reinforced composites and coatings. Metals and their derivatives might not allow the self-healing approach with their relatively high temperature production processes. Methods in self-healing are mostly based on polymeric materials, so the incorporation of self-healing functionality into a metallic material can be very tough because the polymeric adhesives that are used in self-repairing functionality are temperature sensitive. Discovery of new alloys or temperature resistant polymeric materials can enable self-healing functionality in metals.

The focus of this thesis work is solely on the self-healing of polymeric epoxy resin.

Epoxy resin is mostly used as a matrix material because of its unique mechanical properties for composite materials. Cured resin holds fiber reinforcement together and protects them from mechanical and environmental damage. In addition, it has another unique ability which is to transfer the external loads on the reinforcements. In addition to its certain superior properties, it also has some shortcomings. The self-healing ability is crucial in particular for matrix materials having brittle nature such as epoxy, wherein the cross-linked polymer chains do not allow for the orientation of polymer chains. More specifically, when a highly cross-linked polymer is exposed to a critical force, polymer chains crack because of the inability of the chain movement. On the micro scale, these cracked polymer chains are in essence microcracks which may cause premature failure and undesired results for structural polymeric materials. In order for abstaining from an abrupt failure of conventional polymeric materials, microcapsules can be used excellently as a viable repair agent.

In light of the above discussion, the motivation behind this work is to evaluate practicality and feasibility of stimuli-responsive single microcapsule based self healing of epoxy resin used in Resin Transfer Molding process. In regard to the motivation, within the scope of the current MSc study, three goals were set. The first one is to manufacture microcapsule containing healing solution by using in-situ polymerization method and then characterize the produced microcapsules with different spectral and thermal tools. The second one is to embed microcapsules into the thermosetting resin with the purpose of providing the host material of interest with the self healing functionality. Once embedded into the thermosetting polymer, the third goal is to evaluate microcapsules for self-healing functionality through using TDCB specimen. The embedded microcapsules are ruptured upon damage-induced cracking which results in the release of their content into the

crack plane. Toward this end, single-microcapsule based self healing system does not aim to heal base material permanently; on the contrary, project's target is to increase the service life of the base material. In conclusion, microcapsules based self healing approach is hoped to open possibilities for decreasing the intervals of periodic inspection, hence reducing the cost and out of service time of structures.

1.2 Outline of Thesis

The rest of thesis is developed as follows. Chapter 2 briefly summarizes the history of microcapsule based self-healing materials.The performance of the microcapsule based system, production process of different microcapsule systems and fatigue behavior of microcapsule based self-healing epoxy are discussed in Chapter 2. In Chapter 3, a detailed procedure of the encapsulation of water insoluble monomer by the in-situ polymerization of urea-formaldehyde as well as characterization tools for microcapsules and their results are also presented. In Chapter 4,the mechanical evaluation on the thermosetting matrix containing microcapsules is also introduced. Chapter 5 evaluates the self healing functionality of cured epoxy resin. The present work concludes with a discussion of future work in micro capsule based self healing material in Chapter 6

Chapter 2

Background

2.1 Introduction

This chapter provides a reader with relatively comprehensive information on microcapsules with different core and shell material, self healing of epoxy composites as bulk material or adhesive, and fatigue and quasi-static fracture behaviour of self healing materials.

2.2 A Brief History of Self Healing Materials

Within the scope of self-healing concept, Wool and Kim [5] have described the some stages of polymer healing at polymer-polymer interface. These are surface rearrangement, surface approach, wetting, diffusion, and randomization. Wool and Kim [5] have showed that when the two pieces of identical bulk polymeric material were brought into close physical contact above glass transition temperature, the space between them gradually disappeared and mechanical strength at the polymer- polymer interface increased as the crack healed due to the diffusion of polymer chains across the polymer-polymer interface. In this case the chain diffusion at the polymer-polymer seam was a special type of mass transfer which cannot be interpreted by the conventional diffusion equation. To overcome this drawback, they have used microscopic theory of diffusion which is based on the reptation model of chain dynamics by de Gennes. Wool and Kim's theoretical study showed that fracture energy G_{IC}, essentially increases as $G_{IC} \sim t^{1/2}$ and

that the stress intensity factor K_{IC}, behaves as $K_{IC} \sim t^{1/4}$. This theoretical study proved that the stress intensity factor can be used to assess the healing efficiency of bulk polymeric materials. In addition to Wool′s study, de Gennes [6], Jud [7] and Prager [8] also found the same correlation between the fracture energy and healing efficiency of bulk polymers.

After some theoretical work and feasibility analysis, Dry has achieved preliminary experimental study on the vascular based healing system [9]. He fused the millimeter diameter preloaded glass pipettes into epoxy matrix. Glass pipettes were containing either cyanoacrylate or two part epoxy system. His results showed that the delivery of reactive adhesives from the internal pipettes into cracks is way of resisting or stopping further crack growth. The drawback of this study was cyanoacrylate. The solubility of cyanoacrylate in the water and potentially short life of the self-healing agent has led researchers to look for more suitable candidates to meet requirements of the work.

In an independent study of self-healing epoxy matrix, Dry and Mcmillian also tried to incorporate self-healing functionality into concrete [10]. They tried to embed the glass tubes into concrete but the incorporation of liquid-filled glass tubes occasionally failed because of the brittle nature of glass. They overcame this shortage by drilling holes into the concrete. The holes were loaded with three-part methylmethacrylate adhesive system to initiate the crack filling upon damage. Assessment of healing efficiency was done by using the three point bending specimens. Results of this study indicated the crack filling and further flexibility of test sample after the first flexure test. However this study did not contain any specific data about mechanical behavior of drilled samples, since holes can reduce mechanical properties of a bulk material.

Motuku et al. [11] further discovered the usage of different kind of hollow fibers. He assessed compatibility of different kind of hollow tubes when incorporated into fiber reinforced epoxy matrix. They studied the effects of volume fraction and wall thickness of fiber on the matrix impact loading, but they did not evaluate the healing response of composite sample.

Bleay et al. [12] further discovered the hollow micron-scale fibers to enable self-healing functionality of polymer composites. Hollow fibers were filled either epoxy resin or hardener. These fibers provide both self-healing functionality and reinforcing agents to the host material. The content of the fibers was released into

the damaged area, when fibers were ruptured. Compression strength after impact tests were used as a measure of the effectiveness of the repair technique. The discriminating approach of this study was the fluorescent dye through the fibers. Fluorescent dye provided both visual inspection of crack and transport of the reactive fluid into the damaged area.

Kessler et al. [13] has studied manually healing of delamination damage in woven E-glass/epoxy composites. He studied two types of manual healing process. In the first concept, a solution of precatalyzed monomer was introduced manually into the delamination. In the second concept, a self-activated system was created by embedding the catalyst when the composite was manufactured then monomer (DCPD) was injected manually into the delamination. Healing efficiency was calculated approximately 67% for the first concept and 19% for the second concept, in terms of virgin and healed fracture toughness values.

2.3 Microcapsule Based Self-Healing Systems

2.3.1 DCPD-Grubbs Based Approaches

Liquid-filled microcapsules are used in the scope of self-healing materials to separate reactive component from the surrounding matrix. Therefore a living material system which is mechanically and chemically responsive was developed. Various techniques can be found in the literature to prepare microcapsules and microspheres. These techniques can be divided into two groups, chemical methods and physical methods. If these methods are summarized very briefly; the chemical techniques are coacervation, interfacial polymerization, in-situ polymerization, liposomes and inclusion complexation. The physical process can be classified as spray coating, centrifugal extrusion, spinning disk, annular jet, spray drying, prilling, extrusion. Microcapsules were incorporated in the host material as shown in Figure 2.1. When a crack is formed in the host material, microcapsules are ruptured by incoming crack tip and the liquid content of microcapsules is released by a capillary action hence wetting the crack surface. The occurrence of capillary action can be attributed to the compliance difference between matrix and microcapsule wall [14, 15].

In the scope of microcapsule based self-healing system, in-situ polymerization is most commonly used technique to prepare microcapsules containing a hydrophobic core material which will go through the crack plane when the covering polymeric film is cracked[15].

In the first successful microcapsule based self-healing system, dicyclopentadiene (DCPD)-Grubbs' catalyst chemistry was employed. DCPD was encapsulated by the in-situ polymerization of urea-formaldehyde oligomer by using the principle of the oil in water emulsion[16]. DCPD-filled microcapsules were embedded in a thermosetting bulk material with Grubbs' catalyst. In this simple approach Tapered Double Cantilever Beam (TDCB) was used to evaluate the autonomous healing of bulk polymer material. A sharp precrack was introduced to fracture sample to initiate the development of crack during fracture experiment. Once the sample was fractured completely into the two half fragment, then the load was removed. Two piece of beam were brought together and left for healing at room temperature without manual intervention for 48 hours. After the self-repairing process of bulk material, fracture experiment was repeated. Virgin and healed fracture toughness values were determined from the critical load to propagate the existence precrack and fail the specimen. Upon comparing the virgin and healed fracture toughness values, healing efficiency was assessed [14]. In this preliminary study; fracture experiments yielded an average healing efficiency of 60%. In spite of the successful demonstration of microcapsule based self-healing thermosetting system, this study was including some unknown. For instance, there was no information about the tensile or compressive behaviour of self-healing specimen since embedded mixture of microcapsules and catalyst system would decrease the mechanical features of bulk material. In addition, it was pointed out in the study that the kinetics of self-healing and stability of catalyst were two significant shortcomings of this study. When Grubbs' catalyst was added into the uncured resin, Grubbs' catalyst was degraded by the hardener of host material and it was not dispersed well in the Diglycidyl ether of bisphenol-A (DGEBA)-amine system. Low dispersion of catalyst led to incomplete healing of host material [17].

Brown et al. [16] has optimized the encapsulation of DCPD by urea-formaldehyde polymer. He investigated the parameters that affect the encapsulation of DCPD by urea-formaldehyde. The reaction type that was used in their study is the in situ polymerization of urea-formaldehyde at oily phase-water interface. Diameter of microcapsules was controlled by the agitation rates. Ph and interfacial surface

area at the dispersed phase-water interface affected the surface morphology of the capsule shell. On the other hand, shell thickness of microcapsules was independent of agitation rate and manufacturing parameters. For all the batches, shell thickness of microcapsules was in the range of between 160-220 nm. It was found that there is an almost linear correlation between the agitation rate and mean capsule diameter.

Mechanical properties of microcapsules ex-situ were investigated by Keller et al. [18]. By using the single-capsule compression test, elastic modulus and failure behavior of poly (urea-formaldehyde) shelled microcapsule were determined. It was found that average capsule shell wall modulus is 3.7 GPa. Furthermore, they showed that the failure strength highly depended on the microcapsule diameter. As microcapsule diameter decreased, it was found that microcapsule could carry higher load before the failure as compared to bigger microcapsules. In addition, capsule size had no effect on the modulus value which was determined from the comparison with theory. As a conclusion of this study, microcapsules enhance some mechanical properties of host material, such as increasing the fracture toughness value of host material[14, 19].

Kessler [20] studied the cure kinetics of ring opening metathesis polymerization of DCPD. He found that catalyst concentration has significant impact on the cure kinetics of DCPD. As the catalyst concentration increases in the self healing sample, the curing degree of polydicyclopentadiene goes up. He showed that polymerization of DCPD started after first 60 minutes at room temperature. In addition to polymerization time, the degree of polymerization highly depended on the catalyst concentration for first 60 minutes.

Rule [17] has also suggested the encapsulation of the Ruthenium catalyst. To eliminate the some drawbacks of solid catalyst, Grubbs' catalyst particles were encapsulated by the wax. Wax-protected Grubbs' catalyst particles showed good dispersion stability in host material. In addition, wax was not soluble in two part resin system, but it is soluble in DCPD. Hence, during manufacturing of self-healing fracture samples, Grubbs Ruthenium catalyst was not degraded by the curing agent of host material. When the DCPD contacts the wax-protected catalyst, shell of the catalyst was dissolved by DCPD and further ring opening metathesis polymerization of DCPD was achieved in the crack plane.

Mauldin [21] has inspected self-healing kinetics of endo and exo DCPD. Although previous studies have focused on the encapsulation of DCPD and its self-healing

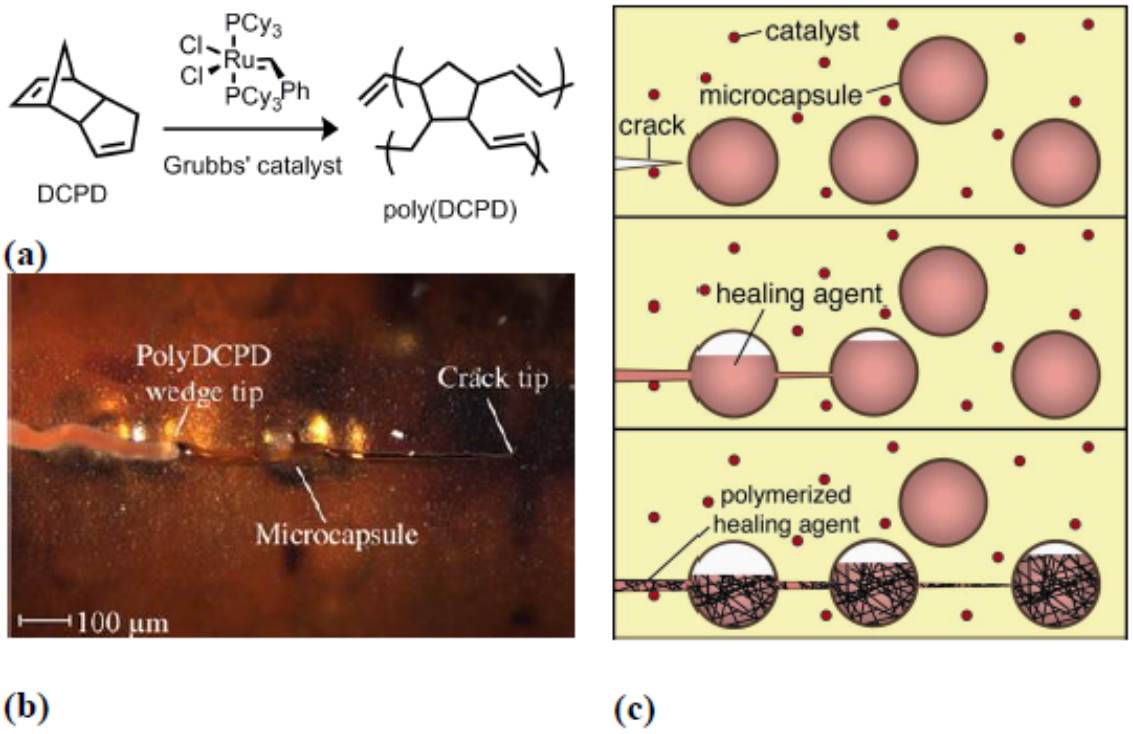

FIGURE 2.1: (a)When endo DCPD contacts with Grubbs' catalyst, a ring opening metathesis reaction takes place at room temperature to form a poly (DCPD). (b) Optical image of in-situ fatigue specimen represent the occurrence of poly DCPD in back of the crack tip. An individual ruptured-microcapsule can be seen. This confirms that an incoming crack break up the microcapsule and content of the microcapsule goes through the crack plane to form poly (DCPD) with Grubbs catalyst. (c) Scheme of autonomous self-healing thermosetting polymer showing crack initiation, rupture of microcapsules and delivery of healing agent into crack plane, and healing agent contact with the catalyst to form a polymer, finally closure of crack plane is achieved[1].

functionality, Mauldin showed that endo and exo DCPD has different self-healing kinetics when used as a healing solution. Two different isomer of DCPD can be seen in Figure 2.2. Exo-DCPD can be polymerized 20 times faster than the endo-DCPD. Faster curing kinetics has led to rapid healing of fracture specimens. On the other hand, rapid healing of fracture specimens caused a significant decrease on the fracture toughness of healed samples. This can be expressed as follow: reduced gel time of exo-DCPD did not allow complete dissolution of relatively bigger wax-protected solid catalyst. Therefore, available solid catalyst was further diminished. As pointed out earlier, weakened catalyst concentration harshly affected the curing degree of polyDCPD. Mauldin et al. optimized the healing kinetics of DCPD as mixing exo- and endo-DCPD. Mixing of exo-stereoisomer and endo-isomer DCPD has led to increased healing efficiency compared to exo-DCPD and also reduced the onset healing time of repairing agent with respect to endo-DCPD.

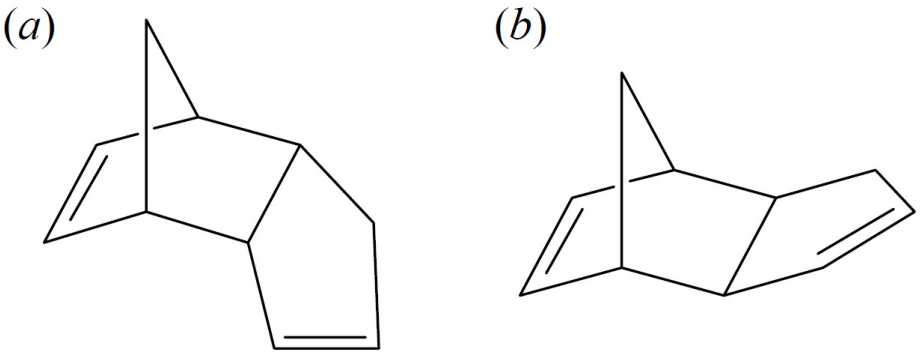

FIGURE 2.2: Chemical structure of a) endo- and b) exo-DCPD

Blaiszik et al. [19] demonstrated the manufacturing of submicron sized microcapsules. He used sonication technique to prepare microcapsule with average diameters as small as 220 nm and as big as 1.65 μm. Microcapsules prepared with sonication technique have shown smooth outer surface. When submicron sized microcapsules were introduced into the epoxy matrix, a small decrease in the elastic modulus and a significant decrease in the ultimate tensile strength were observed. On the other hand, a considerable increase in the Mode-I fracture toughness value was noted. Although, all the superior properties of sub micron size microcapsule incorporated epoxy base material, this study did not show any specific data about the healing efficiency of the any base material.

Kirkby et al. [27, 28] studied self-healing polymers with embedded shape memory alloy (SMA) wires. For a demonstration, shape memory alloy were implanted to the TDCB specimen and different amount of catalyzed monomer were injected to the crack plane manually [27]. It was shown that when SMA wires were activated with an applied current, total crack volume in the fracture specimen was reduced drastically. Therefore, healing of crack can be achieved with a diminished amount of reactive fluid. In addition, a higher healing efficiency was obtained for samples which contain SMA wires. The higher healing efficiency was attributed to the heat generated by the stimulated SMA wires.

Kirkby also showed the in-situ self-healing of thermosetting polymer [28] which both contains the microencapsulated healing agent and shape memory alloy (SMA) wires. Instead of injection of healing agent manually, reactive liquid was encapsulated and introduced the fracture sample during the manufacturing process. As pointed out in previous study, fracture samples which contain the SMA wires showed an improved healing efficiency when compared to the fracture samples that

contained only microcapsules. It was concluded that the fill factor of at least two is necessary to achieve the maximum healing efficiency.

Jin et al. [29] have demonstrated the self-healing of epoxy adhesive. Quasi-static fracture and fatigue behavior of thin film self-healing adhesive were evaluated. This time mechanical performance of self-healing material was assessed by using width-tapered-double-cantilever-beam (WTDCB) specimen geometry, since the base material was thin film (ca. $360\mu m$) instead of bulk polymer. Self-healing constituents were the encapsulated DCPD monomer and first generation Grubbs catalyst particles. The addition of the self-healing components to the neat resin improved the virgin fracture toughness of base material. Quasi-static fracture toughness test indicated recovery of virgin fracture toughness by 56%. Fatigue life of neat and self-healing adhesive was investigated at a maximum stress intensity factor of 0.42 $MPam^{1/2}$ and a stress intensity ratio of 0.1. All the neat epoxy adhesive test specimens failed within 62000 cycles. On the contrary, specimens with self-healing constituents showed a complete crack arrest in the fatigue test.

2.3.2 Alternative Self-Healing Chemistries

Cho et al. [22] incorporated the phase-separated droplets containing hydroxyl end-functionalized polydimethylsiloxane (HOPDMS) and polydiethoxysiloxane (PDES) into the vinyl ester matrix. In this work, the catalyst di-n-butyltin dilaurate (DBTL) was encapsulated by polyurethane polymer and blended to vinyl ester matrix with phase separated droplets. Self-healing behavior of host material was assessed by TDCB specimen through comparing virgin and healed fracture toughness values. When the self-healing components were embedded to host material, a significant increase in the Mode-I fracture toughness value was observed. The healing efficiency of the system was measured approximately 46%.

In a separate study from Cho et al.[23], they studied retardation of corrosion by embedding microcapsules into the metal coating. In this study both healing agent and tin catalyst were encapsulated. He showed a considerable mitigation of corrosion in the metal substrate. Optic and Sem image of self healing coating can be seen in the Figure 2.3.

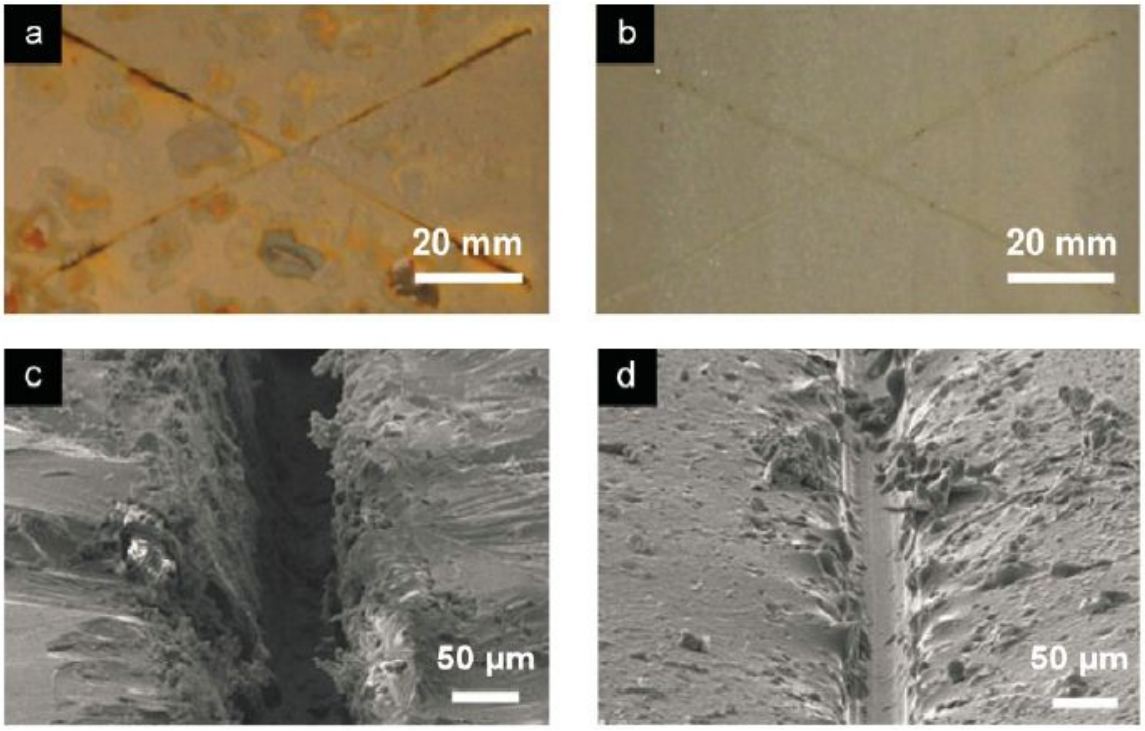

FIGURE 2.3: Morphological evaluation of self-healing coatings. a) control sample b)self-healing sample c) SEM image of scribed region of control sample d)SEM image of scripted region of sample after healed

Kamphaus and his coworkers [24] have examined the use of tungsten (VI) chloride catalyst for ring opening metathesis polymerization of exo-DCPD. The environmental stability of catalyst WCl_6 was poor and it affected further usage of WCl_6 as a catalyst for self-healing application of epoxy resin. Beside the poor stability of the catalyst in the environmental condition, it enabled recovery of mode-I fracture toughness of epoxy matrix. In-situ self-healing of epoxy resin with tungsten (VI) chloride catalyst and exo-DCPD yielded 20% recovery of Mode-I fracture toughness value. As being different from the Grubbs catalyst and DCPD self-healing system, the self-healing constituents which was used in this study depressed the virgin fracture toughness of base material by approximately 48%. The reduction of fracture toughness was attributed to the poor interfacial bonding between catalyst particle and epoxy matrix.

Mookhoek et al. [25] have demonstrated the manufacturing of peripherally decorated binary microcapsules containing two liquids (Figure 2.4). Microcapsules had central liquid which is composed of DCPD and peripherally clothed second microcapsule system around the core. Surrounding microcapsules contained dibutylphthalate (DBP) within the urea-formaldehyde shell with an average diameter of 1.4

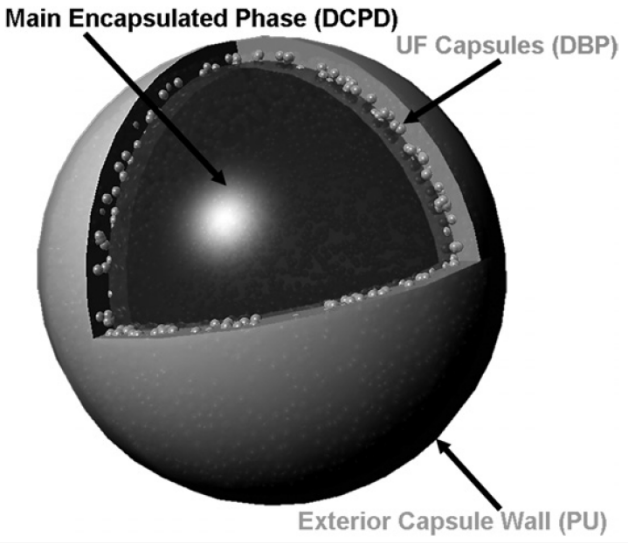

FIGURE 2.4: Schematic representation of binary microcapsule architecture

μm. The binary microcapsule system was manufactured by using DBP microcapsules as Pickering stabilizer without inclusion of surfactant EMA. The binary microcapsules composed of poly urethane as a wall with a mean diameter of 140 μm. Differential scanning calorimetry (DSC) analysis showed a volume fraction of 8.8% DBF in binary capsules. Consequently, a successful method to produce binary microcapsules was developed but the paper did not present any data on the self-healing functionality of any base material.

Mcllroy et al. [30] attempted to encapsulate reactive amine in order to achieve a dual microcapsule self-healing system. In their work, the encapsulation of reactive amine was very problematic due to several reasons. First of all, amine is water soluble and inverse emulsion procedure to encapsulate water soluble compounds was not optimized yet, and also self-healing literature did not present any study on the encapsulation of hydrophilic core until the time of this study. Secondly, attempt to stabilize inverse emulsion caused another phenomena which is called shear thinning. Nanoclay was used to form a Pickering emulsion but it increased the viscosity of continues phase. Finally, the encapsulation was achieved, but no data about the healing efficiency of any bulk polymer was presented. The content of microcapsules was characterized by TGA and titration. TGA indicated a fill factor of 55 wt% for reactive amine-loaded microcapsules.

To eliminate the some drawbacks of DCPD/Grubbs catalyst based self-healing system, Jin and coworkers [31] have both encapsulated epoxy monomer and polyamines to create a dual microcapsule based self-healing system. Encapsulation of epoxy

was achieved following procedure of in-situ polymerization of urea-formaldehyde in an oil-in-water emulsion. Encapsulation of hardener (polyamine) was performed by a novel method. Hardener of epoxy is water soluble thus it cannot be encapsulated by the in-situ polymerization of urea-formaldehyde at the hydrophobic dispersed phase-water interface. Initially, urea-formaldehyde pre polymer was synthesized. The synthesized prepolymer was then placed in a beaker containing only deionized water and surfactant. The solution was agitated vigorously by mixer without oily phase. The significant anecdote of this study was the position of the propeller. The propeller was just fixed beneath of the solution surface in order to entrap air bubbles to the reaction vessel. Therefore, further crosslinking of urea-formaldehyde occurred at the water-bubbles interface and hollow microcapsules were manufactured. Hollow microcapsules were then introduced into a vacuum jar containing liquid polyamine. Jar was vacuumed several hours to provide the transport of amine into the hollow microcapsules. The efficiency of the vacuum infiltration system was low, but it enabled the encapsulation of water soluble phase by the urea-formaldehyde. Dual microcapsule system showed an average 91% recovery of mode-I fracture toughness value for specimen cured at low temperature. When specimens were post cured at 120 $^{\circ}C$ for 1 h, the healing efficiency decreased drastically to 46% and 35% after 8 h post curing. The descent of healing performance was attributed to the diffusion of amine from the capsules at elevated temperature.

Yang et al. [32] has encapsulated the diisocyanate by using the interfacial polymerization of polyurethane(PU). Although isocyanates are catalyst free healing agent, the healing performance of microcapsules containing isocyanates were not evaluated in this study. On the other hand, a detailed encapsulation procedure and characterization methods were presented. The mean diameter of each microcapsule batch showed a totally inverse linear relationship with agitation rate. A power law relation between agitation rate and average batch diameter n= -2.24 was obtained. It was shown that capsule shell thickness changes linearly with the capsule diameter. TGA analysis indicated that capsule fill factor at above 60 wt %. Ex-situ mechanical analysis of microcapsules demonstrated linear elastic compression to failure and increasing average diameter resulted to decline in strength.

2.3.3 Optimization of Delivered Healing Agent into the Crack Plane

Effect of the microcapsule sizes and dimensions of crack faces on the effectiveness of self-healing specimens were investigated by Rule and coworkers [26]. They reduced the crack size of TDCB sample by using a short groove TDCB specimen. TDCB specimen with short groove provided less crack separation for the Mode I fracture test. The relationship between mean microcapsule diameter and mass fraction of the microcapsules was optimized as follow;

$$n = pN \tag{2.1}$$

where n is the number of capsules that are ruptured by a planar crack, p is the probability that the center of capsule lies within the rupture zone of crack plane and N is the total number microcapsules that are available in the test specimen. Supposing that the capsule shell is insignificant (<2% of the capsule diameter), then the probability is written as follow;

$$p = \rho_s A d_c / M_s \tag{2.2}$$

where ρ_s is the density of the matrix, A is the crack area which is formed in the TDCB specimen during fracture test, d_c is the mean diameter of the capsules and M_s is the total mass of the sample. The upper part of the fraction surely indicates the mass of material within in the crack zone. The total number of capsules in given sample can be calculated as follow;

$$N = \Phi M_s / m_c \tag{2.3}$$

where Φ is the mass of capsules for specimen of interest and m_c is the mass of each capsule. The mass of transported healing agent normalized by crack area $\bar{m}$ becomes

$$\bar{m} = m_h / A = n m_c / A \tag{2.4}$$

where m_h is the total mass of healing agent released from the microcapsules to crack plane. The assumption made was that all the microcapsules on the crack

plane was broken during the test. Finally combining the equations (2.1)-(2.4);

$$\bar{m} = \rho_s \Phi d_c \tag{2.5}$$

It can be concluded that the available healing agent in the crack plane is proportional to the weight fraction and mean diameter of the capsules.

2.3.4 Fatigue Studies of Microcapsule Based Self Healing

Brown et al. [2] have done the prelusion fatigue study on self-healing epoxy matrix. The recovery of fatigue life of self-healing specimen under fatigue loading was expressed as follow: λ is the fatigue life extension ratio, N_{healed} is the number of cycles to failure of a self-healing specimen and $N_{control}$ is the number of cycles to failure of a control specimen (without healing materials). The formula can be written as follow;

$$\lambda = (N_{healed} - N_{control})/N_{control} \tag{2.6}$$

As a demonstration, precatalyzed DCPD monomer was injected into the crack plane manually. After the polymerization of premixed monomer in the crack plane, mode-I fatigue crack closure was achieved. A polymer wedge occurred at the crack tip due to the polymerization of injected sample. Formation of the polyDCPD wedge at the crack tip caused a shielding mechanism for fatigue crack. In addition to the fatigue crack closure another phenomena was raised which is hydrodynamic pressure effect of manually injected viscous healing mixture. The hydrodynamic pressure effect retarded the crack growth rate of the mode-I fatigue of TDCB specimen. Consequently a significant fatigue life extension (more than 20 times) was achieved due to formation of the polymer wedge and hydrodynamic pressure at the crack tip. In the second part of this study, Brown and coworkers [33] have investigated in-situ self-healing of fatigue cracks in a microcapsule toughened epoxy composites. Due to the complexity of the in-situ self-healing fatigue study, retardation and successful arresting of fatigue crack was highly predicating on several variables such as applied range of stress intensity factor, rest period, temperature of the rest period, and crack growth rate. The DCPD-Grubbs self-healing system requires approximately 10 hours for full polymerization of monomer at room temperature. Hence the time of failure must be greater than at least 10 hours to

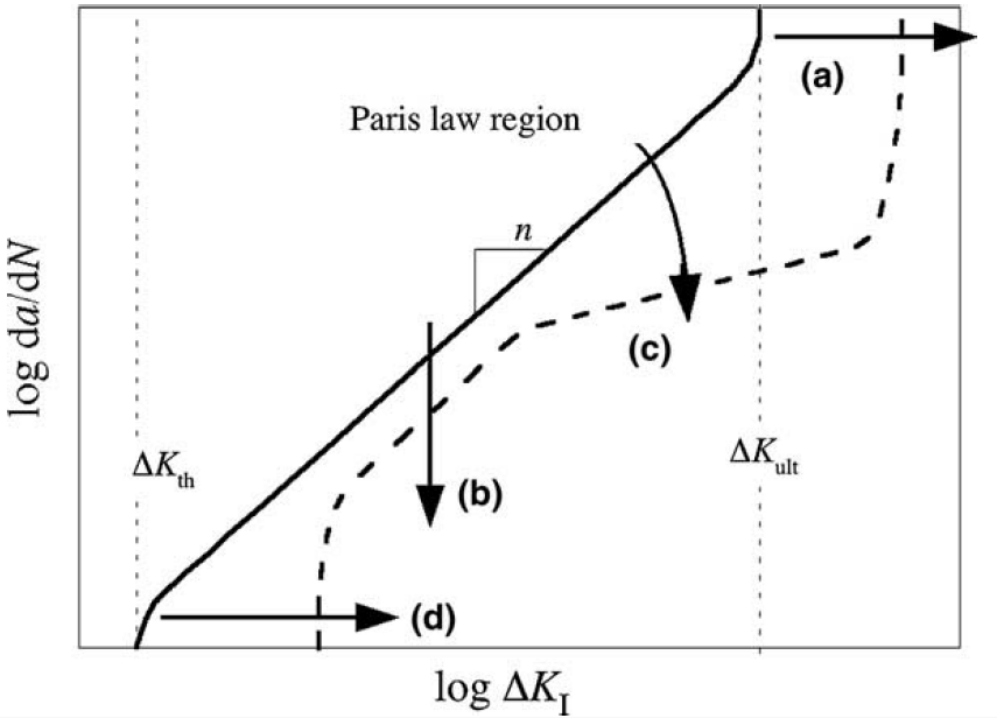

FIGURE 2.5: Representative relationship between fatigue crack growth rate (da/dN) and the applied stress intensity range (ΔK_{IC}) in the Paris power law region. Boosted fatigue behaviour can be obtained by: (a) increasing the range of stress intensity before crack growth instability ΔK_{ult}, (b) reducing the crack growth rate (da/dN) for a given ΔK_{IC}, (c) reducing the crack growth rate sensitivity to ΔK_{IC}, i.e., reduce n, or (d) increasing the threshold ΔK_{th} at which crack growth arrests [2].

observe the fatigue life extension of microcapsule based self-healing epoxy sample. For instance for high $\Delta K_{IC} = 0.7 - 0.9K_{IC}$ values, no life extension was achieved unless a carefully chosen rest period was inserted into the fatigue experiment since $t_{fail} < t_{heal}$. For an intermediate range of $\Delta K_{IC} = 0.5 - 0.7K_{IC}$, the crack propagation has slowed down and resulted with a fatigue life extension, $\lambda = 0.89 - 2.13$ since $t_{fail} \sim t_{heal}$. For small range of ΔK_{IC} such as $\Delta K_{IC} < 0.5K_{IC}$, fatigue experiment resulted with infinite fatigue life-extension. When the $\Delta K_{IC} < 0.5K_{IC}$, no optically measurable crack extension was observed. The high cycle fatigue loading of TDCB specimens has continued seven days. The main drawback of this study was incompatibility between the polyDCPD and epoxy matrix during the fatigue testing of manual injection and in-situ self-healing of TDCB-epoxy specimens. The polyDCPD which is result of polymerized DCPD after the breakage of microcapsule in the crack plane was a hydrocarbon. Therefore intermolecular interactions between the polar epoxy matrix and hydrocarbon polyDCPD was limited. Consequently low interaction between polyDCPD and epoxy seam caused

the debonding of the polyDCPD film from the epoxy matrix during the testing.

Another study was done on the fatigue crack propagation in microcapsule-incorporated self-healing epoxy specimen by Brown and coworkers [34]. Apart from the previous study, they have inspected microcapsule concentration effect on the fatigue life properties. Researchers have found that increasing microcapsule concentration decreases Paris law exponent. In addition to the concentration effect, varying the size of microcapsule did not affect Paris law exponent. Paris law exponent was found 9.7 for neat epoxy specimen and as the microcapsule load rate increased up to 10%, the paris law exponent decreased to the 4.5. The effect of Paris law exponent (n) can also be correlated with Figure 2.5c. The incorporation of microcapsules significantly increased fatigue life of host material for a particular value of $\Delta K_{IC} = 0.586 MPam^{1/2}$. Fatigue life has changed from $86x10^3$ cycles for neat epoxy to $239x10^3$ cycles for microcapsule without rest period.

Jones et al. [35] studied factors which determine fatigue life extension of self-healing thermosetting resin. They found that fatigue life extension of an questioned self-healing specimen was highly depended on the relative mechanics of crack propagation and chemical kinetics of self-healing constitutes. Stress ratio ($R = K_{max}/K_{min}$), frequency (f), and the maximum applied stress intensity ratio (K_{max}) were chosen as mechanical kinetics of fatigue crack growth rate. R and f were kept constant. Therefore K_{max} was the main component of mechanical kinetics. If K_{max} was increased, the crack growth rate, (da/dN) also went up according to the Paris power law,

$$\frac{da}{dN} = C(K_{max} - K_{min})^n \tag{2.7}$$

When the kinetic of chemical reaction between self-healing constitutes was increased, the greater Mode I fatigue life extension was achieved. As recrystallizing the Grubbs catalyst, researchers have improved reaction kinetics of self-healing compounds. On the other hand this time another phenomenon raised. The faster dissolving morphology is also more susceptible to deactivation resulting from the exposure to amine-based epoxy curing agents. They solved this problem by wax encapsulating the recrystallized solid bis-tricyclohexylphosphine benzylidene ruthenium (IV) dichloride catalyst. The recrystallized and wax encapsulated catalyst has increased the rate of polymerization of liquid DCPD fourfold. The improved polymerization rate has extended the fatigue life of questioned self-healing polymer over 30 times higher than a non-healing specimen. On the other hand fatigue

life of epoxy polymer under high crack growth rate can only be expanded through the substitution of carefully timed rest periods.

Keller and coworkers [36] also studied mode III torsional fatigue behavior of self-healing - PDMS (polydimethylsiloxane) elastomer. PDMS resin was diluted with heptane, followed by encapsulation of urea-formaldehyde polymer. Initiator was encapsulated as received. Healing compounds were embedded in PDMS host material and the healing mechanism under the fatigue cycle loading was examined. Their result indicated that significant torsional stiffness recovery was achieved and total crack growth was reduced by 24%.

2.4 Concluding Remarks

In the scope of microcapsule based self healing materials, different kind of repairing agent and catalyst have been used. Yet optimal self healing materials have not been obtained due to self healing kinetics of constitutens, degradation or availability of catalyst, incompability between healing agent and matrix. Recently it was shown that encapsulation of diglycidyl ether of bisphenol-A (DGEBA) is the most promising candidate for microcapsule based self-healing materials. On the other hand, the catalyst of DGEBA make this material problematic for the self-healing approach. There are several attempts to encapsulate liquid phase amine to provide polymerization of repairing agent when capsules get ruptured whereas encapsulation of liquid phase amine indicates some limitations. These limitations are mostly based on aging of amine loaded capsules [30, 31]. Liquid amine-loaded microcapsules can lose their integrity in a several months. When base material is cured at elevated temperature, liquid amine-loaded microcapsules lose their activity hence cause a decrease in efficiency of self healing system. To increase their shelf life different encapsulation procedure and wall material is needed. The problem of microcapsule containing amines is mostly due to the leakage of capsule content during the post curing of samples at elevated temperature. If the double walled microcapsules containing amine-based curing agent is produced, the leakage problem might be eliminated somehow. In addition, it is necessary to change wall material of DGEBA loaded microcapsules with non-toxic material because of some health and environmental issues.

Several microcapsule-based self-healing systems for polymers have been reported in the literature, including DCPD/Grubbs catalyst, DCPD/tungsten hexachloride (WCl_6), PDMS/dimethyldineodecanoate tin (DMDNT) catalyst, PDMS/Pt catalyst, epoxy/mercaptan, and epoxy/boron trifluoride diethyl etherate ($(C_2H_5)_2OBF_3$). DCPD/Grubbs catalyst system performed well but unfortunately this approach has several shortcomings. First of all, DCPD is a toxic compound, and inhalation of it may causes several damage in the human body [37]. In addition availability of Grubbs catalyst is very limited. Encapsulation of PDMS seems problematic [22] when literature is investigated, it can be seen that PDMS has some curing problem when used as a healing agent. Epoxy/mercaptan and epoxy/dimethyldineodecanoate also have some curing problem when utilized for self-healing application. Moreover their shell consists of urea-formaldehyde and exposure to formaldehyde is a significant consideration for human health [38].

Chapter 3

Microcapsule Preparation and Characterization

3.1 Introduction

In this chapter, we have explained the production of microcapsules which is employed for producing self healing composite materials for the present work. Additionally, a detailed characterization of microcapsules are presented.In the first section of this chapter, microencapsulation of hydrophobic core is presented with a detailed experimental conditions. Thereafter, optic image and size distribution of each microcapsule batches are provided. In the fourth section, thermal analysis data (TGA and DSC) of each microcapsule batches are given along with a detailed explanation. In the fifth part, a detailed chemical characterization of microcapsule in the mid-IR spectra is presented followed by a final remark on this chapter.

3.2 Manufacturing of Microcapsules

Microcapsules containing an oily phase was produced by using the in-situ polymerization of urea-formaldehyde, following the method defined by Blaiszik et al. [39]. The microcapsules stores diglycidyl ether of bisphenol-A (DGEBA) with a solvent chlorobenzene (PhCl). Due to the relatively high viscosity of the core compound ($\eta_{DGEBA} = 1.3Pas$), the encapsulation of DGEBA alone by urea-formaldehyde within the water was not possible. Therefore, PhCl which is a non-polar solvent

FIGURE 3.1: A microencapsulation set-up

with rather low viscosity value ($\eta_{PhCl} = 0.75x10^{-3}Pas$) have been used to decrease the viscosity of main core component, thereby enabling the encapsulation of specimen of interest.The microencapsulation set-up can be seen in Figure 3.1. At room temperature, 100 ml deionized water and 25 ml %1.5 wt/v aqueous solution of ethylene maleic anhydride copolymer (EMA) were mixed in 250 ml beaker. The beaker was placed in a temperature controlled silicon oil bath with an external thermocouple (VELP SCIENTICA Magnetic Stirrer and Digital Thermoregulator). The solution was agitated with a programmable digital mixer (Heidolph RZR 2102) to obtain a fine emulsified dispersed phase. A digital mixer propeller (a three- bladed axial marine type propeller with the blade diameter of 25 mm) was placed at bottom of the reactor.

As agitation continues, 2.5 gr CH_4N_2O(urea), 0.25 gr NH_4Cl (ammonium chloride) and 0.25 gr $C_6H_6O_2$ (resorcinol) were added the solution. After the wall material is dissolved in solution, approximately fifteen minutes later, the ph of the solution was measured to be around 2.7 then, it was raised to 3.5 through the drop-wise addition of the NaOH (sodium hydroxide). The 30 ml DGEBA+PhCl mixture was very slowly added to the solution. Before the addition of the core material, 15 ml DGEBA and 15 ml PhCl were mixed in a 50 ml beaker to decrease the viscosity of DGEBA to the desired viscosity range for the encapsulation. Upon the

addition of the core material, an emulsion was formed. To stabilize the dispersed phase, the emulsion was subjected continuous agitation under the mechanical stirrer for approximately 15 minutes. Due to the high shear rate in the reaction vessel, emulsion droplets tend to break down hence reaching to a stable size. The stabilization of emulsion droplets is achieved by the help of the surfactant EMA. 6.68 gr formalin aqueous solution of 35 % wt formaldehyde was added to the emulsion after the given stabilization time.

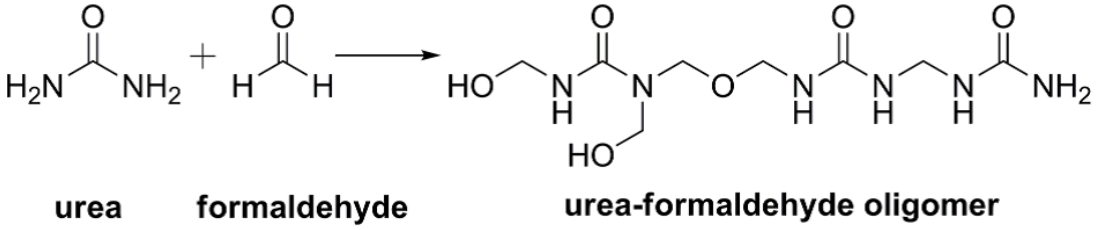

FIGURE 3.2: Polymerization of urea and formaldehyde to form short chain oligomers that make up the shell walls of microcapsules (reaction conditions = 4 h at 55 $°C$, pH 3-5)

Therefore, a molar ratio 1:1.9 between formaldehyde to urea was achieved [40]. The reaction schema between the urea and formaldehyde can be seen from the Figure 3.2. The emulsion was covered with an aluminum foil and heated at a rate of 1 $°C/min$, up to 55 $°C$. The reaction has lasted for 4 hours with continued agitation at 55 $°C$. After 4 hours of continuous agitation, the mixer and heater were turned off. Additional approximately 100 ml of deionized water (55 $°C$) was supplied to suspension. After suspension reached the room temperature, the microcapsule slurry was filtered and washed several times with deionized water and dried in the hood for 36- 48 hours. Then, it was dried in a vacuum oven at 30 $°C$ for 24 hours.

After successful fabrication, filtering and eventually drying of all microcapsule batches, the yield of the each batch was measured by using a sieve with 500 μm hole size. Processing chart of microcapsules can be seen in Figure 3.3. Final microcapsule samples were poured in sieve and sieve was shaken and finally the particles which successfully passed through the sieve was considered to be a final product. The particles which did not pass through the sieve were not used in the calculation of the yield. The yield was determined by dividing the mass of particle which successfully pass through the sieve to the mass of microcapsule material used for synthesis. The yield of each microcapsules batch was calculated by using following equation;

$$yield = \frac{the\ mass\ of\ microcapsule\ that\ passes\ the\ sieve}{the\ mass\ of\ reactants} \tag{3.1}$$

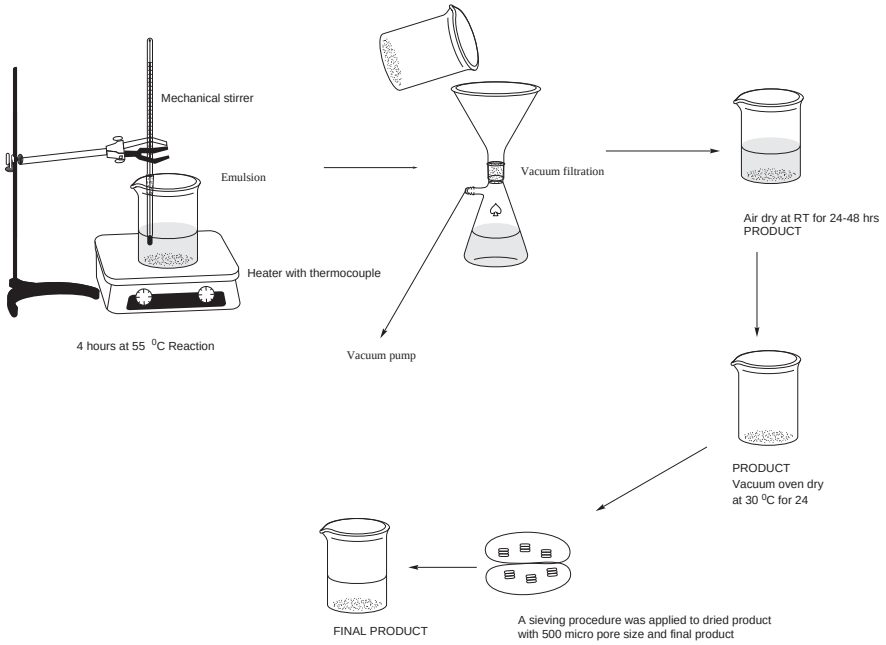

FIGURE 3.3: Processing chart of microcapsules; encapsulation reaction of DGEBA, filtering of microcapsules from aqueous medium, air-dry, drying in vacuum oven to remove excess water , sieving with $500\mu m$ sieve, final product

3.3 Optic Image of Microcapsules

An optical microscope(Nikon ECLIPSE ME600) has been used to take the optic images of urea-formaldehyde walled microcapsules containing hydrophobic core material. The optic image of four different microcapsule batches can be seen in the Figure 3.4. All images were taken either at 5x or 10x magnifications. Small amounts of dried microcapsule powder were poured in a petri dish containing mineral oil. A good dispersion of microcapsules in mineral oil was achieved by shaking the petri dish several times. The mineral oil bath was used to separate the individual microcapsules from each other since microcapsules tend to stick together. By changing the location of the petri dish with a manual carrier, at least 100 microcapsule images were obtained from a different region of petri dish for each batch. The size of microcapsules were measured using the image analysis software (Spot Advanced Version 4.6).

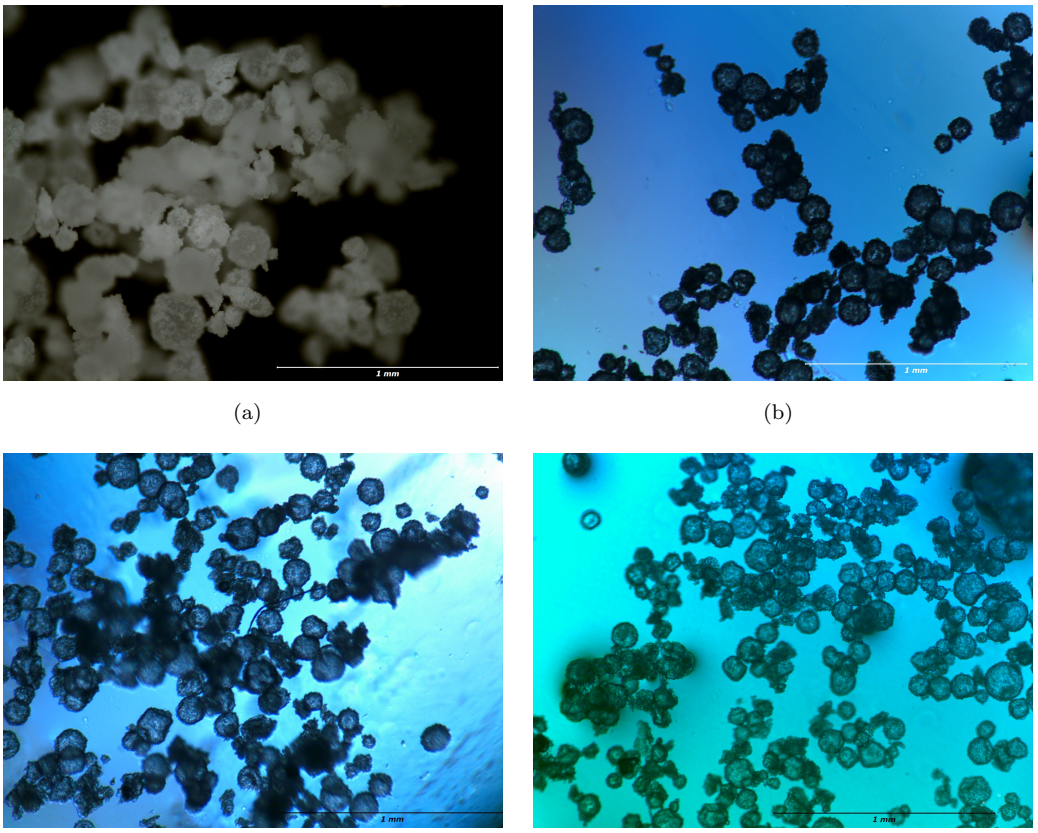

(a) (b)

(c) (d)

FIGURE 3.4: Optic microscope images of microcapsules;(a) at 467 rpm, (b) at 556 rpm, (c) at 643 rpm, (d) at 706 rpm,

3.4 Size Distribution of Each Microcapsule Batches

The mean microcapsule diameter was calculated for each microcapsule batch by finding the mean value of total measurements. It is clear that when the agitation rate increases, the diameter of microcapsules decreases. This proportional decrease can be seen in the Table 3.1. The relationship between batch diameter and agitation rate can also be seen more clearly in Figure 3.6. This decrease is due to the relationship between shear rate and droplet size as described by Taylor[41]. Even though a logical correlation exist between agitation rate and shear rate, the bearing with Taylor's study is relatively far away for our work since in our reactor, fluid flow around the propeller is turbulent rather than laminar considered by Taylor. In addition to the relationship between droplet size and agitation rate, another connection between the agitation rate and standard deviation can be established. It can be concluded from Figure 3.6 that the higher agitation rates, the

smaller the standard deviation for each of the microcapsule batches. Our results were consistent with the literature.

To see the effect of agitation rate on the size distributions of all capsule batches, bar diagram of each batches were plotted, which can be seen in Figure 3.5. It is clear that when the agitation rate increases, the interval of the microcapsule size range decreases. A clear relation between the agitation rate and yield can not be obtained. Nevertheless, it is desirable to say that when the agitation rates increases, the final product of microcapsule powder sticks together rather than being freely flowing powder. This sticky behavior affects the yield since some agglomerated microcapsule particles can not pass the sieve. Furthermore, a proportional decrease in standard deviation with increasing agitation rate can also be seen in Table 3.1. The formula used to calculate standard deviation is as follow;

$$STDEV = \left(\frac{1}{n-1} \sum_{i=1}^{n} (x - \bar{x})^2 \right)^{\frac{1}{2}} \tag{3.2}$$

where x is the sample mean, n is the sample size, and $\bar{x}$ is individual microcapsule size values

TABLE 3.1: Agitation rate, mean diameter, standart deviation, and yield

ID	Agitation rate (rpm)	Mean diameter(μm)	Standart deviation	Yield(%)
C1	467	201.8	39.4	30
C2	556	119.6	21.3	43.7
C3	643	114.4	25.3	39.4
C4	706	96	21.4	-
C5	800	78.5	13.7	18.3
C6	900	53.1	9.1	27.8

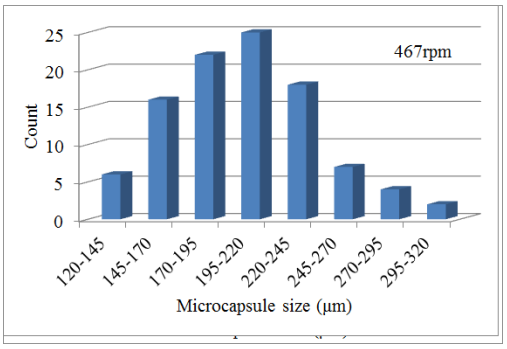

(a)

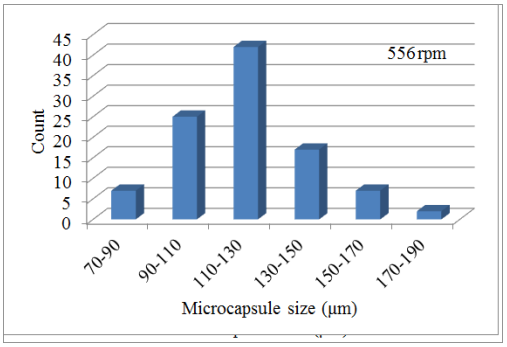

(b)

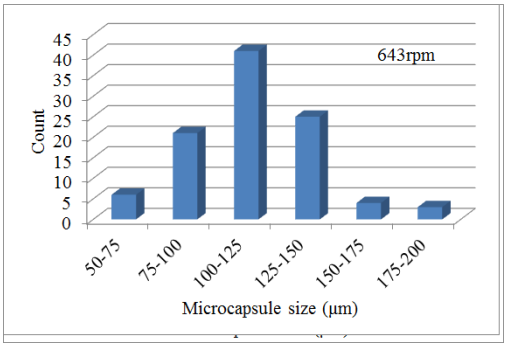

(c)

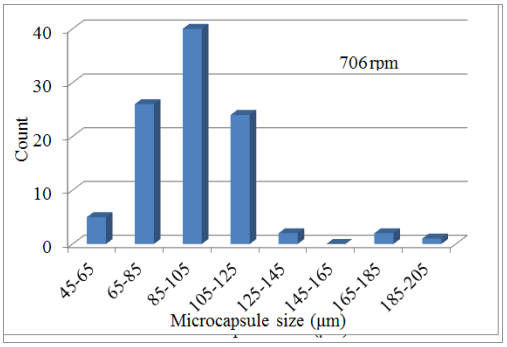

(d)

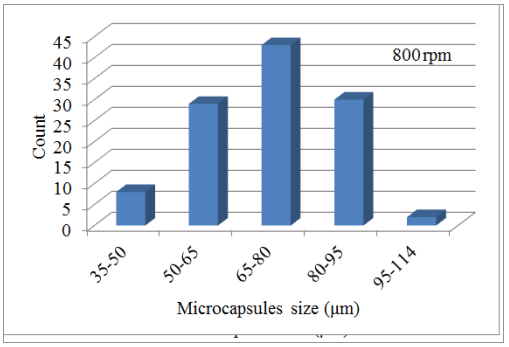

(e)

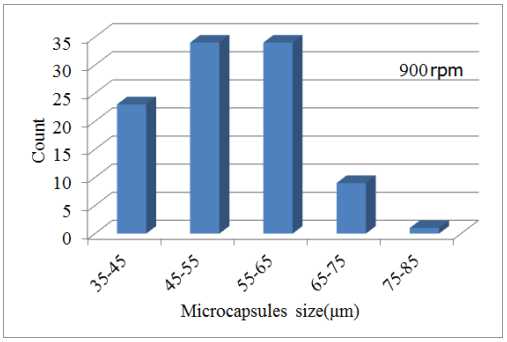

(f)

FIGURE 3.5: Bar diagram of six different microcapsule batches;(a) at 467 rpm,(b) at 556 rpm, (c) at 643 rpm, (d) at 706 rpm, (e) at 800 rpm, (f) at 900 rpm,

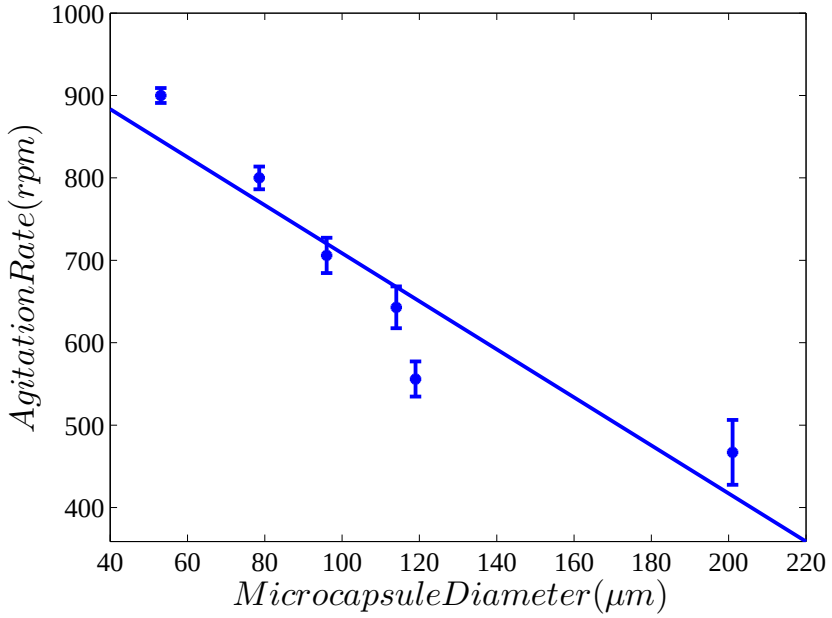

FIGURE 3.6: Agitation rate versus mean batch diameter

3.5 Thermal Analysis

Microcapsules containing diluted DGEBA were produced according to the method mentioned above. Thermal stability of each capsule batch was assessed by Thermogravimetric Analyser (TGA) (Netzsch STA 449 C). TGA is a thermal characterization method wherein changes in some physical and chemical properties can be measured as a function of increasing temperature. In this technique, material is heated with a constant heat rate while the decomposition of material which is usually interpreted by mass loss is computed as a function of time or temperature. Hence, TGA can be used as quantitative technique since it gives a characteristic decomposition temperature of materials. Approximately 10 mg of dried microcapsule powder was weighted from each batch in a ceramic crucible to see the characteristic decomposition temperature of microcapsule constituents. The crucible was placed in a STA. The sample was scanned in a controlled nitrogen atmosphere at 10 $^{\circ}C/min$ ramp rate from room temperature to 500 $^{\circ}C$ while mass loss trace was simultaneously recorded with a software.

Figure 3.7(a) renders the TGA trace of neat UF resin. In Figure 3.7(a), mass loss around the 210 $^{\circ}C$ is due to the decomposition of urea-formaldehyde cross-linked polymer. Moreover, this characteristic decomposition temperature can be

easily seen in Figure 3.7(c), but this time, the decomposition temperature of UF is displaced to 240 $°C$. Figure 3.7(c) represents the TGA trace of six different microcapsule batches. The slight difference between decomposition temperatures of neat UF resin and UF wall which covers microcapsules can be seen in Figure 3.7(a) and 3.7(c). Figure 3.7(b) shows that the TGA trace of neat core material which is composed of PhCl and DGEBA. Before thermogravimetric analysis of core material, PhCl and DGEBA were mixed in terms of equivalent weight ratio to simulate the microcapsule core material because prior to the encapsulation reaction, these two compound were mixed in the same weight ratio. In Figure 3.7(b), characteristic decomposition temperatures of both PhCl and DGEBA can be seen. The decomposition starting around the 130 $°C$ belongs to PhCl while the one around the 350 $°C$ is for DGEBA. Figure 3.7(b) also indicates that PhCl and DGEBA have the same weight fraction in TGA trace. In Figure 3.7(c), constituents of microcapsule which are UF wall material, and DGEBA can be seen. The reason why PhCl can not be seen in the Figure 3.7(c) is due to the low decomposition temperature of PhCl which is around 130 $°C$, meaning that during the decomposition of shell of microcapsules, chlorobenzene also breaks down. Therefore, it is hard to determine PhCl content in microcapsules because one can not distinguish the PhCl and UF wall material from the Figure 3.7(c). As mentioned earlier, the point around 350 $°C$ shows the decomposition temperature of DGEBA (Figure 3.7(c)). Therefore, mass fraction of DGEBA can be determined from the TGA trace. The amount of DGEBA in six different microcapsules batches is between 60-85%.

The other interesting point of TGA trace is the effect of the agitation rate to the DGEBA percentage in microcapsules samples. It is clear that when agitation rate increases, the amount of DGEBA also increases, as seen in Figure 3.7(c). Conversely, the percentage of urea-formaldehyde, which is the shell compound of the microcapsules, decreases. The decrease in the amount of wall material can be associated with the individual diameter of the dispersed phase. It is obvious that when the shear rate increases, the mean diameter of the emulsified phase decreases. When the diameter of the dispersed phase decreases, so also does the surface area of the individual droplets. The smaller surface area provides a smaller interfacial surafce to deposit the urea formaldehyde nano particle. Therefore, a diminished amount of urea-formaldehyde nanoparticle accumulates the dispersed phase-water interface, as seen in Figure 3.7(c).

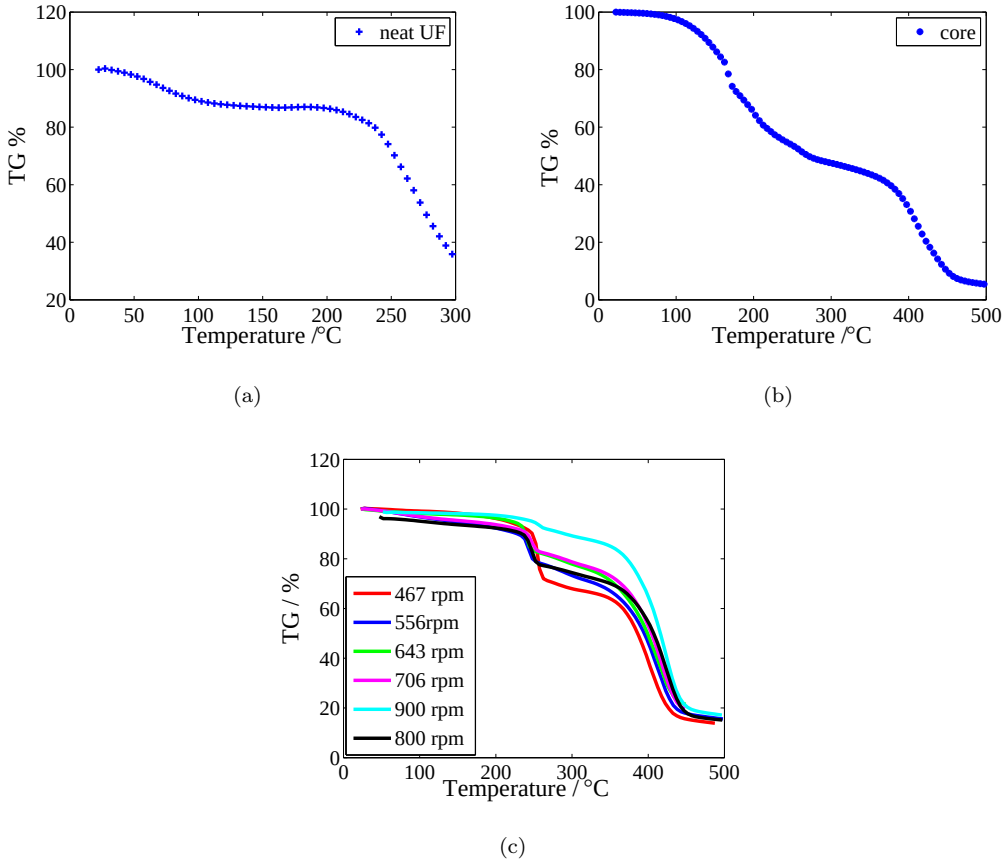

FIGURE 3.7: TGA trace of (a) neat UF resin, (b) core material of microcapsule, and (c) six different microcapsule batches

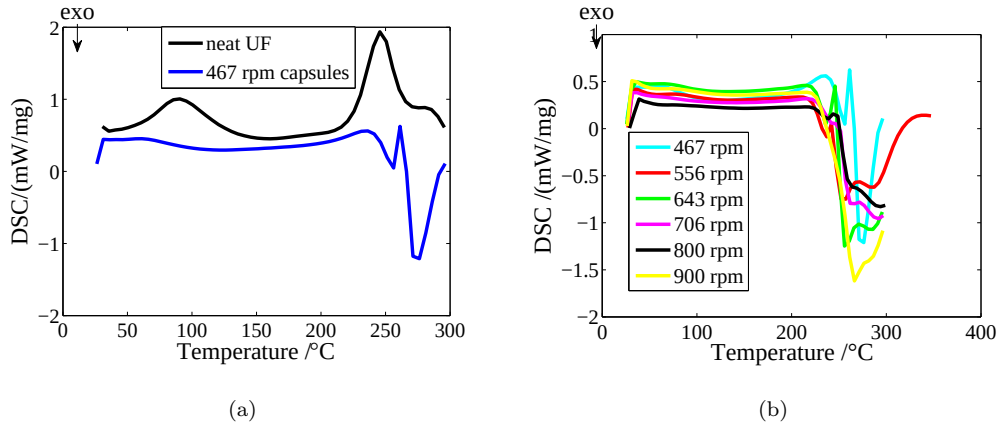

FIGURE 3.8: DSC trace of (a) one particular capsule batch, and (b) six different capsule batches

Differential scanning calorimetry (DSC) analysis also indicates the encapsulation of DGEBA by the urea-formaldehyde shell. DSC analysis of six different microcapsule batches can be seen in Figure 3.8(b). Nevertheless, it is still very hard to mention about chlorobenzene content in microcapsules. On the other hand, it is expected that the chloronzene should be inside the microcapsules. As mentioned earlier, the viscosity of DGEBA does not allow for the encapsulation of the emulsified phase by urea-formaldehyde. It is obvious that DGEBA was mixed with PhCl before adding to the reaction chamber. In addition, PhCl is a non-polar organic solvent and thus, is not soluble in water. Moreover, PhCl is miscible with the DGEBA. Finally, PhCl must be in the dispersed phase with DGEBA in emulsion and one should expect that the emulsion droplets were encapsulated by urea-formaldehyde. The endothermic peak around 240 $°C$ as seen in Figure 3.8(b) is the decomposition temperature of urea-formaldehyde[42]. The exothermic one in Figure 3.8(b) at about 261 $°C$ might be due to the rapid exothermic polymerization reaction of core material, which is triggered by the gaseous products such as ammonia, monomethylamine and trimethylamine yielded by the decomposition of shell materials. The exothermic peak at about 260-270 $°C$ on DSC curves may be due to the continuous polymerization reaction of core material.

The heat flow difference between one microcapsule batch which is prepared at 467 rpm and neat UF resin also can be seen in Figure 3.8(a). In Figure 3.8(a), the endothermic peak of neat UF resin around 90 $°C$ can be attributed to decomposition of free formaldehyde.

3.6 Chemical Analysis

The wavenumbers range 500-4000 cm^{-1} are called mid infrared region (mid-IR) (2.5-20 μm) and it usually gives significant information about the fundamental vibrations and associated rotational vibrational structure of chemical bonds. The mid-IR region is the spectral region where most of the fundamental spectral information is produced.

The chemical bond analysis of all microcapsule batches and sample of interests were done by using IR spectrometer (Thermo Scientific Smart iTR Nicolet i510). Attenuated total reflection (ATR) mode of IR spectrum was prepared. The background was collected from 32 scans between the ranges of 500-4000 cm-1. When

the background scan was completed, tip of ATR was unclamped and microcapsules samples or compounds of interest were placed on the ATR crystal. The tip was clamped against to ATR crystal to provide more intimate contact of the sample with the evanescent wave so that trapped air is not in the medium in which the evanescent wave travels. If the tip is not clamped against the ATR crystal, trapped air can distort the results. After ensuring the adequate condition for Mid-IR measurement of capsules samples or compounds, the scan was initiated. A total of 32 scans were collected from each sample. The background was extracted and Mid-IR spectra of each microcapsule batches or compounds were obtained. The results are given in Figure 3.9.

Mid-IR spectrum of mono chlorobenzene (PhCl) can be seen in Figure 3.9(a). The peaks at 3070 and 1475 cm^{-1} come from the C-H stretching vibration of the phenyl ring. The other characteristic transmission peaks of chlorobenzene are about 1020 and 680 cm^{-1}. These peaks are C-H in-plane and out of plane bending vibration of phenyl ring respectively[44].

Characteristic FTIR peaks of DGEBA, which is the main component of the microcapsules can be seen in Figure 3.9(b). The peak which is around 3050 cm^{-1} is the C-H stretching of epoxide ring. This is the characteristic peak of DGEBA, since DGEBA has terminal oxirane groups. The characteristic transmission peaks of DGEBA at about 1610 and 1509 cm^{-1} are the stretching C=C of aromatic rings and C-C stretching vibration peaks of the aromatic, respectively in DGEBA [43]. Other characteristic transmission peaks of DGEBA are about 1227, 910 and 830 cm^{-1} and they are associated with C-O-C stretching vibration of epoxide ring [43].

The Figure 3.9(c) shows the Mid-IR spectra of the neat urea-formaldehyde thermosetting polymer. The reaction condition of the synthesized neat urea-formaldehyde is the same as that of diluted DGEBA-loaded microcapsules. The neat shell material was synthesized at 467 rpm and the ph of the reaction was kept at 3-4. During the chemical reaction between urea and formaldehyde, they become a cross-linked polymer. The cross-linked urea-formaldehyde polymer can be interpreted from the broad band which is about 3350 cm^{-1}. This peak corresponds to the characteristic of NH and OH functional group.

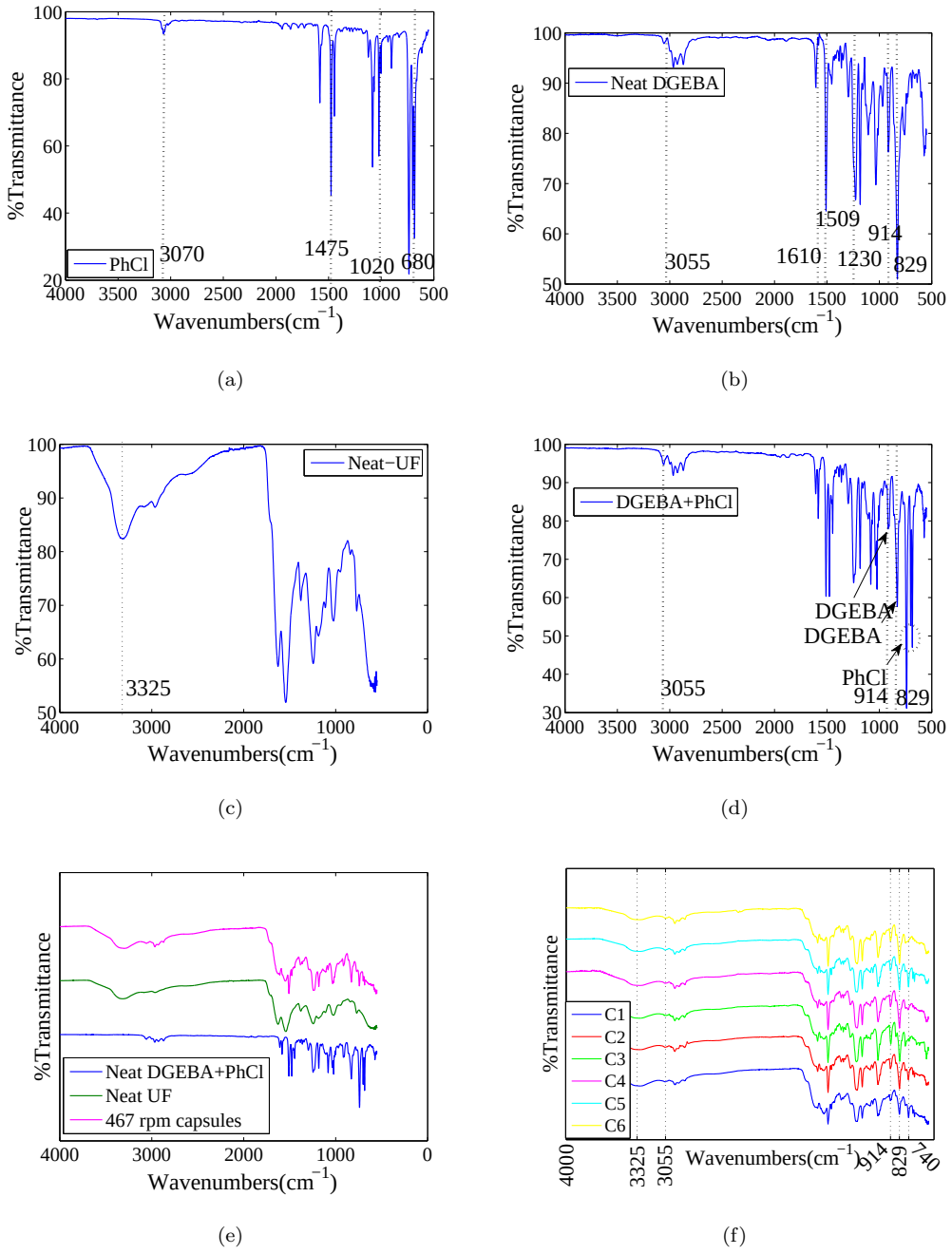

FIGURE 3.9: Mid-IR spectra of;(a) UF resin, (b) DGEBA, (c) PhCl , (d) core material, (e) core material and UF resin, and (f) all capsule batches

In Figure 3.9(d), mid-ir spectra of core solution can be seen. To investigate the Mid-IR spectra of the core material, DGEBA and PhCl were mixed at the same ratio which was defined previously. The IR spectra of the core solution shows characteristic peaks of core compound. Three characteristic peaks of chlorobenzene between 740, 700, and 680 cm^{-1} still exist and can be used to determine the

chlorobenzene content in the each capsule batches. The C-O-C stretching vibration of the epoxide ring (829 and 914 cm^{-1}) can be utilized to show the existence of DGEBA in the each of the microcapsule batches.

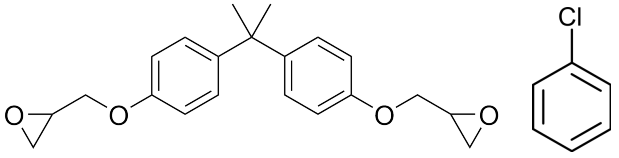

(a) (b)

FIGURE 3.10: chemical structure of (a)DGEBA, (b) PhCl

Moreover, the C-H stretching of the epoxide ring (3055 cm^{-1}) is still strong and this peak can be used to characterize the DGEBA content in microcapsules.

Figure 3.9(e) compares mid-IR spectra of the core content of microcapsule, the shell of the microcapsules, and a batch of microcapsule which is prepared at 467 rpm. Each compound has its own characteristic IR peaks. Therefore, it is logical to use the Mid IR spectra of microcapsules to show the existence of both the core solution and the UF wall material.

Mid-IR spectrum of each of the microcapsule batches can be seen in the Figure 3.9(f). Experimental conditions are the same for six different microcapsule batches except for the agitation rate. The agitation rate just controls the one of the physical property which is the mean diameter of the microcapsule batch. Therefore agitation rate does not affect the chemical composition of the microcapsule batches. All the microcapsule batches have the characteristic peaks of both core and wall material. The characteristic peaks of PhCl (740,700,680 cm^{-1}), DGEBA (829,914 and 3055 cm^{-1}) and urea-formaldehyde oligomer (3325 cm^{-1}) can be easily seen from the Figure 3.9.

3.7 SEM Image of Microcapsules

Surface morphology of microcapsules were examined by scanning electron microscopy(SEM,Gemini). First of all, a carbon tape was mounted on a conductive stage, then microcapsule samples were placed on the carbon tape. Microcapsules

were sputtered with a thin layer of carbon in a carbon coater to prevent charging under accelerated electron beam. SEM sample holder with microcapsules was placed on the SEM stage. Image of the microcapsules were then taken under different magnifications with an accelerated voltage rate of 2 kV. Microcapsule shell has rough morphology on the outer surface as shown in Figure 3.11. The rough outer surface can be seen in the Figure 3.11(c) and Figure 3.11(d), and this rough outer surface promotes the bonding of microcapsules to the host material. This rough surface is due to the agglomeration of urea-formaldehyde particle as shown in Figure 3.11(a)

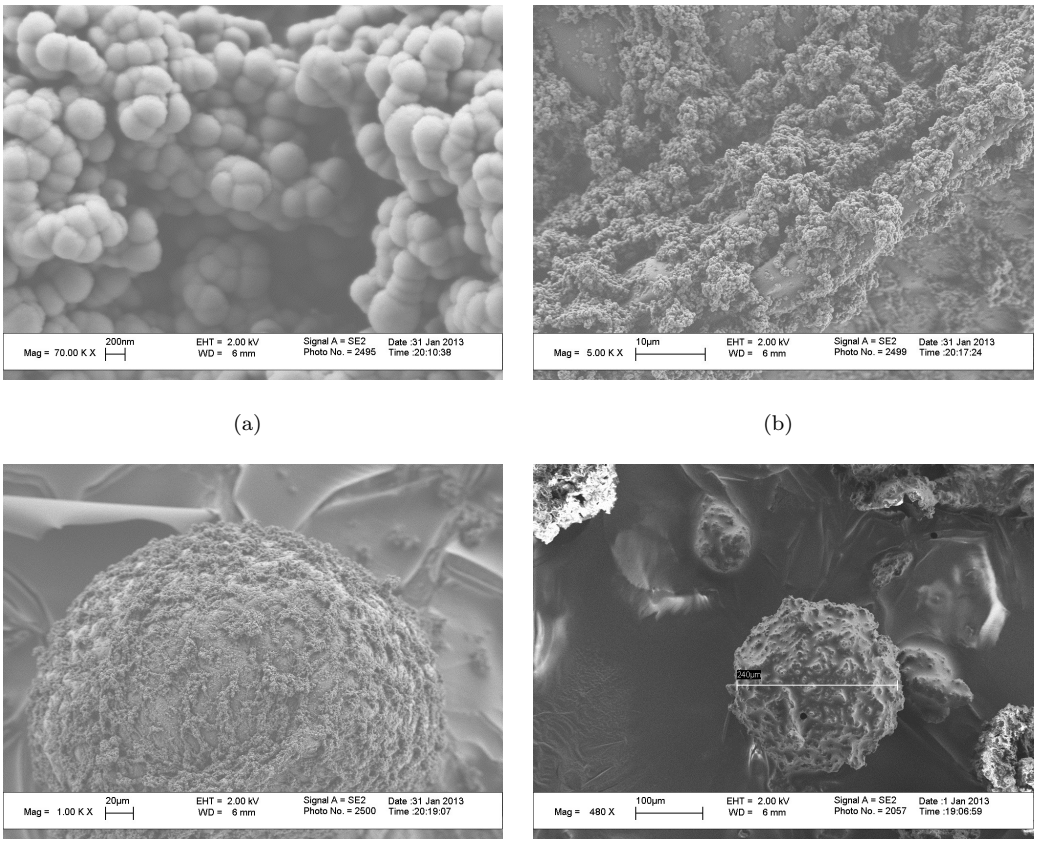

(a) (b)

(c) (d)

FIGURE 3.11: SEM image of;(a) a microcapsule outer surface(at 70 KX),(b) outer surface of same microcapsule (at 5 KX) , (c) same microcapsule, and (d) another microcapsule,

3.8 Conclusion

Solvent promoted DGEBA microcapsules were successfully produced by the in-situ polymerization of urea-formaldehyde on the water-emulsified phase interface. Their chemical characteristic was obtained by Mid- IR spectrum. It was shown that Fourier Transfer Infrared Spectroscopy (FTIR) can be used as a qualitative technique to determine composition of microcapsules. As well, it is a non-destructive testing method and does not cause any material lose during the analysis. The thermal behavior of each microcapsule batches was evaluated by a Thermogravimetric Analyzer. The results have indicated that microcapsules are thermally stable up to 250 $^{\circ}C$. Microcapsules which is produced with above described method can be used in real applications since in real applications, structural materials get heat treatments and the temperature of this heat treatment is usually around 100 $^{\circ}C$.

Controlled agitation rates experiments show that the mean diameter of each of the microcapsule batches can be controlled by the agitation rates in a certain diameter range.

Theoretically, the core of the microcapsules should be composed of 50 % of DGEBA and 50 % of PhCl in terms of weight ratio, since prior to emulsification process, DGEBA and PhCl were mixed in a same weight ratio and poured in a reaction vessel. On the other hand, the TGA trace indicates that the DGEBA content is considerably higher than the PhCl in microcapsules. According to the TGA trace, the DGEBA content of each microcapsule batches is between 60-85 % in terms of weight percentage. The other 15-40 % weight percentage of microcapsules then must belong to shell and PhCl content. It is hard to say about the percentage of the shell and the PhCl in microcapsules from the TGA trace, since PhCl has a boiling point at 130$^{\circ}C$ and it cannot pass the shell of the sphere until the decomposition point of urea-formaldehyde resin (250 $^{\circ}C$). Finally, when the temperature of the crucible reaches the 250 $^{\circ}C$, both the shell and PhCl decompose. It is impossible to determine the amount of PhCl in microcapsules from the TGA trace. On the other hand, the Mid-IR spectra indicates the existence of chlorobenzene in microcapsules.

Chapter 4

Fracture Experiment

4.1 Introduction

Following the successful production of microcapsules in a lab scale in chapter 3, in this chapter, the ability of microcapsules for microcrack repairing in epoxy matrix is investigated. The experimental setup and procedure are explained along with the governing equations utilized for evaluating the fracture toughness value of self healing composites. The preparations of fracture sample and silicon rubber mold are described. In the first section of this chapter, the quasi-static fracture procedure is detailed. Thereafter, mold and fracture specimen fabrications are explained. Finally, test results and fractography are presented.

4.2 Quasi-Static Fracture

Linear Elastic Fracture Mechanics (LEFM) has a theoretical basis in that all energy dissipation is associated with the fracture process and the deformation occurs in a linear elastic fashion. This approach covers the brittle failures in polymers. The macroscopic response of a brittle polymeric material subjected to mechanical load can be seen in Figure 4.1. LEFM consider that linear elastic body includes a sharp crack and then describes the energy change which happens when such a body undergoes an increase in the crack area. The crack should be already existed in material for LEFM approach. The most fundamental parameter of fracture is

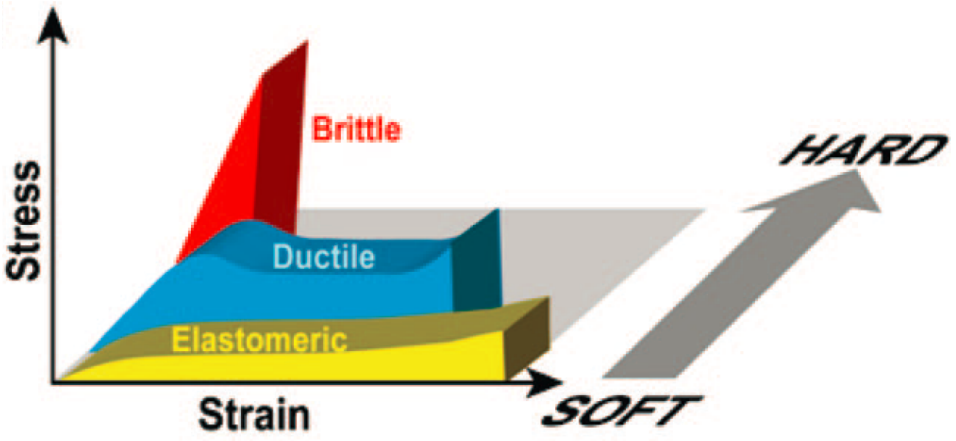

FIGURE 4.1: The macroscopic response of polymeric materials subjected to mechanical load is generally described by a stress-strain curve [1].

the Energy Release Rate, G, which is defined as the rate of energy released by the crack growth [45],

$$G = \frac{dU}{dA} \tag{4.1}$$

where dU is the energy change and dA is the area increase. In the light of LEFM, it is desirable to consider our epoxy matrix as a brittle material since during the mechanical tests, it follows linear elastic fracture behavior. For example, during the mode-I fracture test , breaking occurs with a limited strain. This can be explained as follow; during the Mode-I fracture test, all the energy is consumed by the mechanism that initiates crack formation and overall deformation of material becomes negligible. Therefore, after the breakage of the material, it is easy to bring back the fracture surfaces. When fracture surfaces comes back almost their initial position, the healing at polymer-polymer interface can be achieved more successfully.

In the framework of LEFM approach, tapered double cantilever beam (TDCB) geometry can be used because it meets the several important requirements to characterize microcapsule based self healing. First of all, after the breakage of the specimen into two half pieces, it provides adequate surface area to both halves, when they are brought together. Secondly, this test geometry provides almost controllable crack growth. Thirdly, it is a crack independent measurement of fracture

toughness when compared with the double cantilever beam (DCB) specimen. Finally. TDCB test protocol follows the same procedure which was done early days of the self healing materials that when two cracked surfaces of same material are brought back at above the glass transition temperature, and the interface between them is gradually disappeared and healing of polymer seam is achieved cite [5].

After recognizing the superior attributes of TDCB specimen, now, we need to derive the equation that governs the TDCB geometry. The TDCB geometry has a height profile h, and thickness b. The force P is applied by pin grips and is perpendicular to the direction of crack growth. The general geometry of the TDCB specimen which is used in our work was developed and verified by Beres et al. [46] and modified by Brown et al. [47]. By suitable choice of the TDCB geometry, the change in compliance becomes constant with respect to crack length. It is desirable to start from energy balance for strain energy release rate for TDCB specimen;

$$P\frac{d\delta}{da} + \frac{dE}{da} = \frac{dW}{da} + \frac{dK}{da} \tag{4.2}$$

where E is the energy in the system and W is the work done by the system. δ is the cross head displacement and K is the kinetic energy. The energy balance equation can be simplified by assuming that the test frame equipment that is used during the mechanical testing has negligible compliance, so the derivative of cross-head displacement δ with respect to change in crack dimension is zero. The stable crack growth is the other essential concern of this test procedure. Therefore, the change in kinetic energy with respect crack length can be assumed to be zero (dK/da). The formula can written as follow,

$$\frac{dE}{da} = \frac{dW}{da} \tag{4.3}$$

During Mode-I fracture testing of TDCB specimen, the elastic energy is released by development of new fracture area, meanwhile the derivative of energy term with respect to crack area (dE/dA) also gives the strain (elastic) energy. If Δa is considered an incremental crack augmentation, then a newly created crack area

becomes $\Delta A = \Delta a b_n$, where b_n is the thickness of the TDCB specimen at the crack plane. Therefore strain energy becomes

$$G = \frac{dE}{dA} = \frac{da}{dA}\frac{dE}{da} = \frac{\Delta a}{\Delta A}\frac{dE}{da} = \frac{1}{b_n}\frac{dE}{da} \tag{4.4}$$

Equation (4.3) implies the energy in the sample of interest which is equal to work done on the sample. In addition, work can be calculated as an area under the load -displacement curve because our epoxy system is a brittle polymer and the fracture of our resin system follows the linear elastic definition of strain energy. Therefore, $W = (1/2)P^2\delta$, and C=δ/P_c then $W = (1/2)P^2C$, where C(a) is the compliance of the TDCB specimen with respect to crack length [48]. Strain energy can be rewritten as follow,

$$G = \frac{1}{b_n}\frac{dW}{da} = \frac{1}{b_n}\frac{d}{da}[\frac{1}{2}P^2C(a)] = \frac{P^2}{2b_n}\frac{dC}{da} \tag{4.5}$$

and the derivative of the compliance with respect to precrack length is given [48] as

$$\frac{dC}{da} = \frac{24a^2}{Ebh^3} + \frac{6}{Ebh}(1 + \frac{\nu}{2}) \tag{4.6}$$

Substituting equation (4.6) back into equation (4.5) gives

$$G_{IC} = \frac{8P_c^2}{2Eb_nb}m \tag{4.7}$$

where

$$m = \frac{3a^2}{h^3} + \frac{6}{8}(1 + \frac{\nu}{2})\frac{1}{h} \tag{4.8}$$

In conclusion, the measurement of the strain energy release rate requires knowledge of only the critical load at fracture P_c, the Young's modulus E, and the geometric constant m. The stress intensity fracture toughness is then easily obtained from the strain energy release rate in equation (4.7) as

$$K_{IC} = \sqrt{G_{IC}E} = 2P_c\sqrt{\frac{m}{b_n b}} \tag{4.9}$$

The equation can be reduced to two variables since the terms m, b_n, and b are constant for the given geometry. The equation becomes

$$K_{IC} = \alpha P_c \tag{4.10}$$

The constant α is used to represent m, b_n, and b.

4.3 Fabrication of TDCB Specimen

TDCB specimen was utilized to evaluate the self healing ability of host material with embedded microcapsules. The modified dimension of TDCB [47] was modeled by using a 3-D drawing program. To enable the controlled crack growth mechanism, the side grooves was inserted to the geometry.

The specimen thickness is fixed to 6.25 mm outside of the crack plane and 2.5 mm in the crack plane. The long edge of the specimen is 76.2 mm and short edge of the specimen is 61 mm. The specimen's V-notch side grooves has an angle 45° and the length of 59 mm. The thickness reduction in the crack plane is equal to 60 % ($b_n/b = 0.4$). The distance from the load line to the end of specimen is 79.3 mm. For the specimen shown in Fig. 4.2, $\alpha = 11.2x10^3 m^{-3/2}$ for crack lengths varying from 20 to 40 mm [48].

When design was completed, the model of geometry was machined by a CNC machine tool from Aluminium. The middle section of the specimen where v-notch side grooves are located were manufactured by a computer controlled line erosion machine. The diameter of the line which is used by line erosion machine is 250

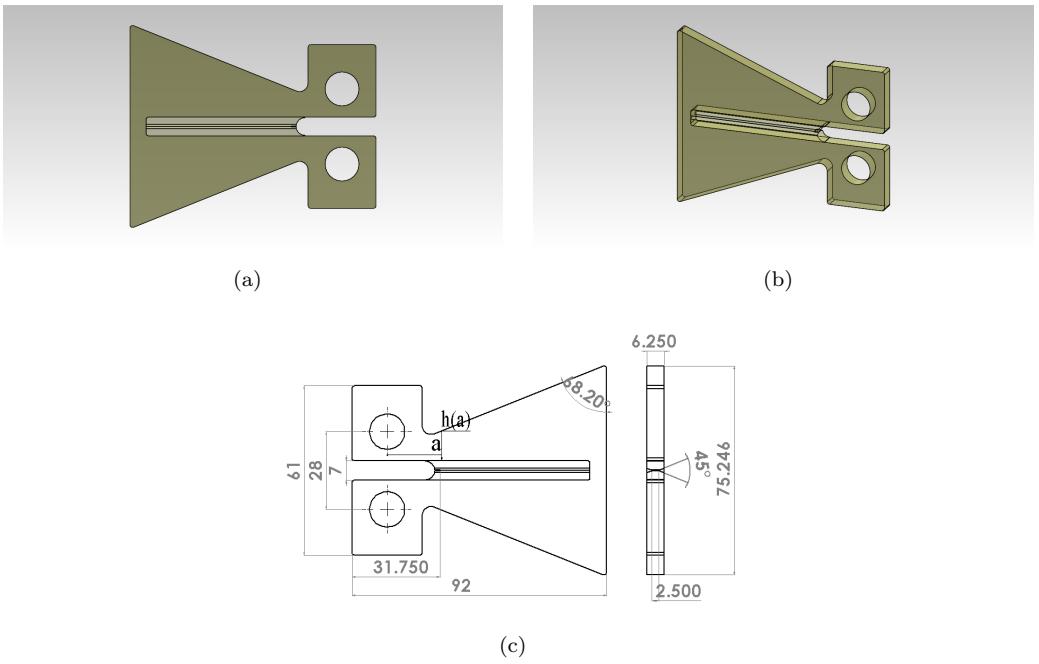

FIGURE 4.2: Solid drawings of TDCB specimen,(a)front-view, (b) trimetric view, and (c) Some basic dimension (mm) of the self-healing test specimen

μm. If the diameter of line is neglected, because it left 0.25 mm radius in the grove planes, therefore, planes of the side grooves are connected each other with a sharp angle of 45°

By using the Aluminium model of TDCB geometry, several silicon-rubber moulds were manufactured in our laboratory. Moulds were composed of two different parts. One type of mould was only utilized to create middle part and the other one was used to create whole specimen. The self-healing part of the TDCB fracture specimen is cured at 50°C for 15 h, then it was placed into silicone main mould for manufacturing TDCB specimen and two-part resin system is prepared with the ratio of 100:36 by weight, degassed in a vacuum jar and poured into the main silicone rubber mould. The sample is cured at 50°C for 15 h. Note that while curing the TDCB fracture specimen, the middle part gets additional heat treatment at 50°C for 15 h. Figure 4.3 shows the preparation and testing stages of fracture sample.

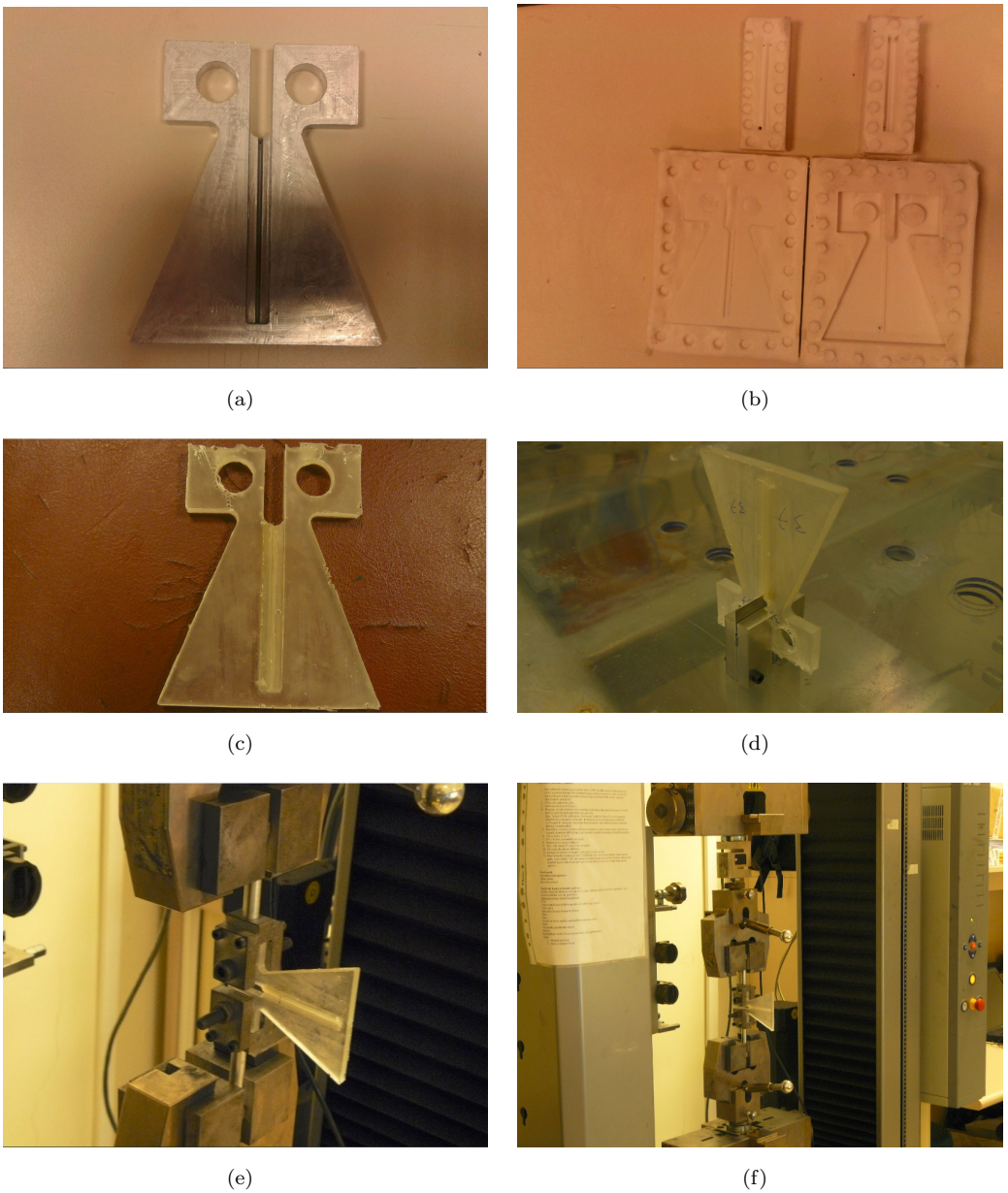

(a) (b) (c) (d) (e) (f)

FIGURE 4.3: (a) Main aluminium model of TDCB geometry, (b) Silicon-rubber moulds, (c) Test specimen, (d) introducing a precrack, (e) image of specimen with testing apparatus and blue mark indicates the end of precrack, and (f) image from testing

4.4 Fracture Experiments

All the mechanical fracture experiments in this study have been done under quasi-static loading in which the samples were loaded monotonically. A sharp precrack was introduced gently by tapping a razor blade into the molded starter notch in the samples. The length of virgin precrack was varying from 22 mm to 43.5 mm for

all TDCB specimens used in fracture tests. Fracture experiments are conducted on two different samples, namely the samples with and without microcapsules in the central region of the specimen. The samples without any microcapsules have been used as control samples while those with microcapsules in the crack plane have been prepared and used for testing in-situ self healing mechanism of system of interest.

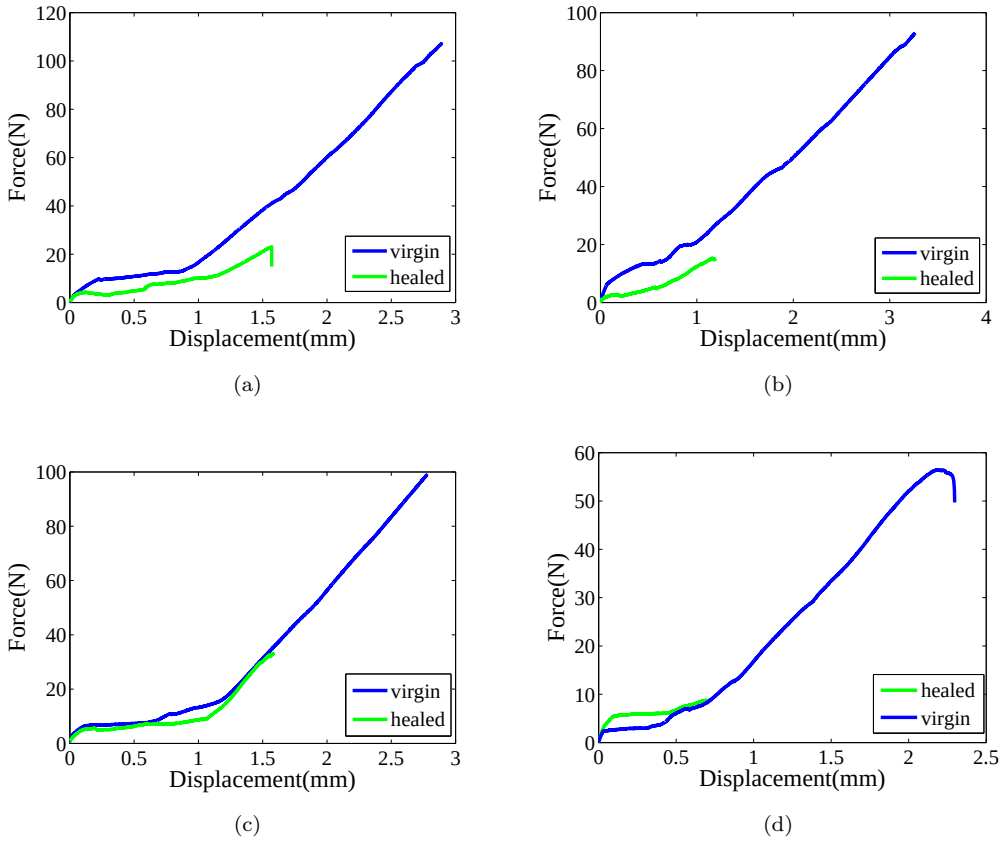

FIGURE 4.4: (a)-(d) Force-displacement curve for four different self healing specimens

After creating a sharp precrack, the TDCB specimens were pin loaded and tested to the failure using a Zwick/Roell Z100 static test machine with a 10 KN load cell under displacement control at a rate of 300 $\mu m/min$. After the failure of the specimens, defined as the complete breakage of the sample into the equivalent two half pieces, crack faces were brought together and left in a temperature controlled oven to ensure the further cross-linking of the healing agent inside the crack plane. The result of the some fracture tests are presented in Figure 4.4. Even though fracture samples are subjected to heat treatment after virgin fracture toughness experiment, second fracture results indicate low self-healing efficiency. The self

healing efficiency is described as a ratio of healed fracture toughness value to virgin fracture toughness. Fracture toughness value $K_{IC} = \alpha P_c$ of TDCB specimen is only dependent on geometric constant α and critical force P_c which is the force to propagate an existing precrack. When values of virgin and healed fracture toughness values are taken, geometric constant α cancels and healing efficiency which is the ratio of the healed and virgin fracture toughness values becomes only dependent on virgin and healed critical forces.

An interesting result of the fracture toughness experiments is the toughening mechanism observed. The fracture experiments have showed that when microcapsules are incorporated into the fracture specimens, the critical load at fracture increased noteworthily. The fracture toughness value of self healing specimens increase 30.4% in comparison to the neat epoxy sample. Table 4.1 shows the difference of fracture toughness value between the self-healing sample and neat epoxy sample. The average critical load at fracture for neat epoxy resin is 97.00 N. This result almost perfectly agree with the manufacturer data[49] since $K_{IC}=\alpha P_c$. The increase in the fracture toughness value can be attributed to crack pinning effect [50] as mentioned earlier since in the crack plane, significant crack tail formation can be seen (Figure 4.6(g) and Figure 4.6(h)).

TABLE 4.1: Effect of microcapsules on the virgin TDCB peak load and fracture toughness K_{IC}

	Virgin Peak load (N)	K_{IC}(Mpam$^{1/2}$)
Manufacturer	-	1.05
Neat epoxy-TDCB	97.00	1.09
TDCB with microcapsules	129.00	1.44

4.5 Three Point Bending Experiments

Compression experiments were done by using Zwick Z100 test frame. The flexural properties of neat and self-healing epoxy resin were investigated by utilizing ASTM D-790-3 standards [51]. Epoxy resin was mixed with the hardener at the ratio of

100:36 by weight with or without capsules, and then the resin mixture was degassed and poured into the open teflon mould. All samples were cured at 50 $^{\circ}C$ for 15 hours. At least 5 different specimen were tested from the each series of samples. Rate of cross head motion was set to 13.6 mm/min to meet ASTM D 790 criteria. The support span, thickness of the specimens and width of specimens were set to 50 mm, 3 mm and 14 mm, respectively. Result of three point study can be seen in Figure 4.5. As can bee seen from the figure, as the mean diameter of the microcapsules increases, the flexural strength of the samples decreases almost linearly.

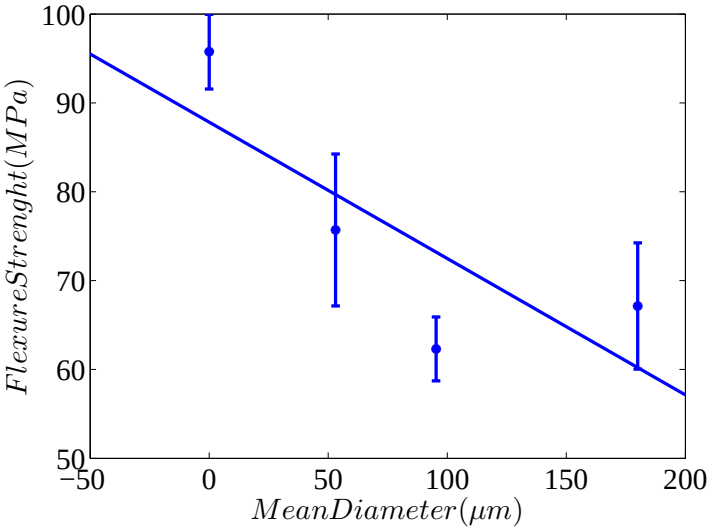

FIGURE 4.5: Mean Diameter versus Flexure Strength

4.6 SEM Images of Fracture Surfaces

Scanning electron microscope(Gemini,Leo-SUPRA 35VP) was used to image fracture surface of samples with a 2-5 kV electron source after sputter coating with a carbon or gold source. Image of fracture surface was taken with different magnification. SEM images indicate that during fracture of self healing samples, microcapsules were ruptured and their content was released into the crack plane. Holes in the crack plane also confirm that during fracture test, incoming crack ruptured microcapsules that lies within the rupture zone of crack plane. Fracture surface of six different self-healed samples can be seen in the Figure 4.6(a)-Figure 4.6(f).

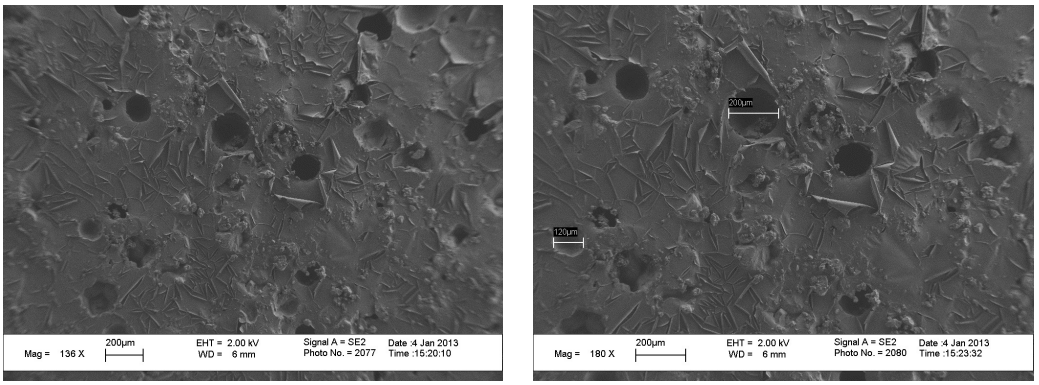

(a)

(b)

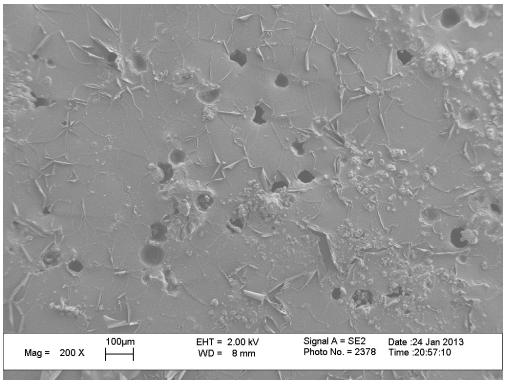

(c)

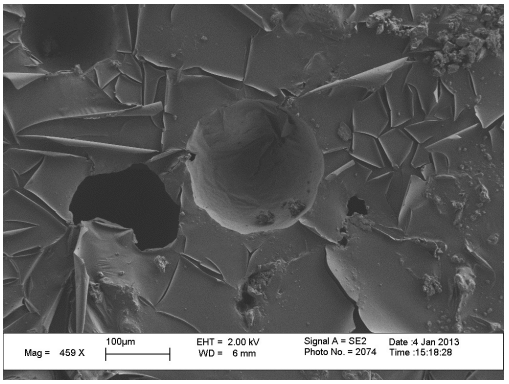

(d)

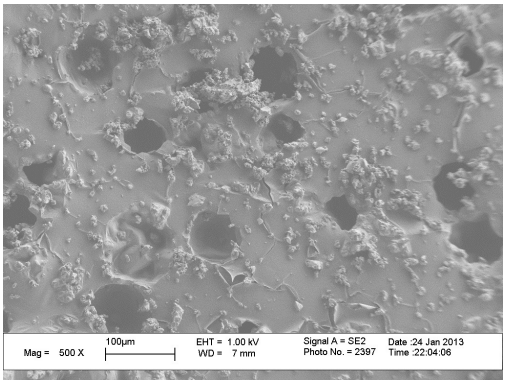

(e)

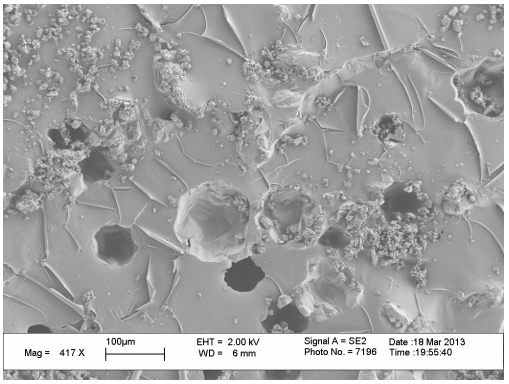

(f)

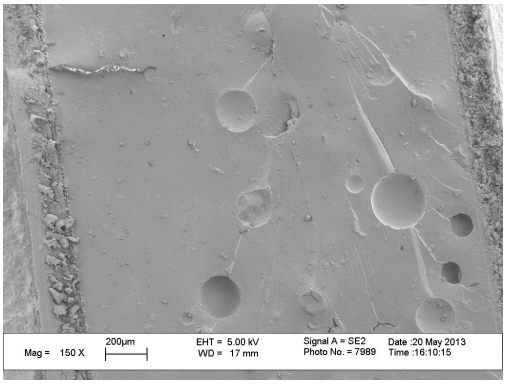

(g)

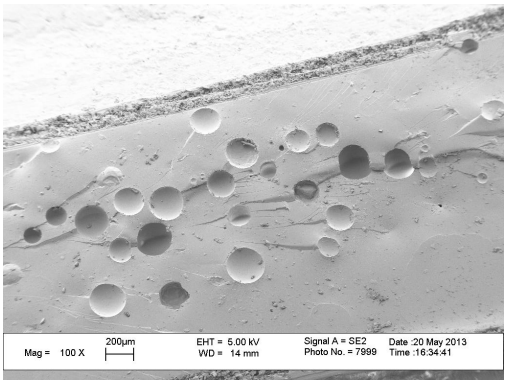

(h)

FIGURE 4.6: (a-f)SEM images of healed surface after second breakage,(g,h)unhealed surface and tail formation

Chapter 5

Results and Discussion

The overall objective of this work was to investigate and evaluate the intrinsic self-healing ability of epoxy resin, which could be achieved through incorporating microcapsules containing epoxy resin and PhCl into an epoxy resin based host material.In this work we define our self-healing system as a semi-intrinsic self healing system because self healing system benefit from incorporated second phase which are microcapsules and natural matrix. In this semi-intrinsic self-healing approach, the microcapsules that render selfhealing functionality to the host material are composed of a microencapsulated epoxy healing agent and the catalyst for the curing of the encapsulated epoxy resin is provided by the un-reacted amine groups in the host. The healing process is activated such that due to the external loading applied on the host materials, the pre-crack is propagated therein, which can easily rupture the rather brittle wall of microcapsule whereby the encapsulated healing agent leaks into the crack zone or plane, and thus reacts with the un-reacted amine groups in the host material. The local curing process in the vicinity of the crack zone due to the reaction of the amine groups with the healing agent takes place, leading to the repair of the damaged zone. It is therefore expected that the self-healed sample would regain its structural integrity and strength albeit not being as high as the virgin structure. It has been observed that due to the relatively high cure temperature of the host material, the amount of un-reacted amine groups would be lower. This results in the lack of catalyst in the crack plane, which decreases the healing efficiency of the intrinsic self-healing process drastically. To this end, the results of the mode-I fracture test have indicated small healing efficiency even though the samples were healed at relatively high temperatures for a long period of time. The reason behind the relatively low healing efficiency in the

semi-intrinsic self healing process is due to the lower amount of un-reacted amine or catalyst in the crack plane. This short coming of the semi-intrinsic self healing process can be circumvented through embedding catalyst-loaded microcapsules in the host material along with the healing agent loaded microcapsules. In this case, since the incoming cracks would rupture both encapsulated the healing and the catalyst solution simultaneously, the lack of un-reacted amine groups in the crack zone would be no longer a problem, and both healing agent and the catalyst would be able to react to initiate local cross-linking of healing solution in the crack plane. This work is original due to the fact that to the author best knowledge, it is the first study that addresses the semi-intrinsic self healing ability of the RTM purpose epoxy resin system in the literature.

The other important point of our work was the TDCB specimen. This specimen was utilized to evaluate self healing functionality and the efficiency of the system. At the early stages of the current work, we have produced and tested TDCB specimens without grooves and the results of these efforts have clearly indicated that it is essential that the TDCB specimens should have grooves to be able to conduct consistent mode-I fracture test. The existence of grooves in the TDCB specimens guarantee a controlled crack growth through preventing the crack from deviating from its direction, and ensuring that it propagates perfectly perpendicular to the direction of the applied load. The difference in the crack growth pattern for TDCB specimens with and without grooves can easily be noticed from Figure 5.1

The preparation of microcapsules is one of the most important stages in the process of self healing study on thermosetting polymer since microcapsules store the reactive material and alienate them from the surrounding environment until the self-healing process is triggered, upon which, the microcapsules release their content into the crack plane. Therefore, the successful synthesis of microcapsules constitutes the fundamental part of the current work, which was performed utilizing the principle of in-situ polymerization of ureaformaldehyde. The work performed on the synthesis of microcapsules has indicated that a variety of non-polar solvents can be encapsulated by using in-situ polymerization of urea-formaldehyde. To show the encapsulation of a non-polar solvent, PhCl was also encapsulated using the same principle. Optic image and mid-IR spectra of PhCl-loaded microcapsules can be seen in the Figure 5.2. According to Figure 5.2(a), three characteristics peaks of PhCl which are 740, 700, and 680 cm^{-1} can be seen. This three characteristic peaks ensure the encapsulation of PhCl. In addition to FTIR analysis,

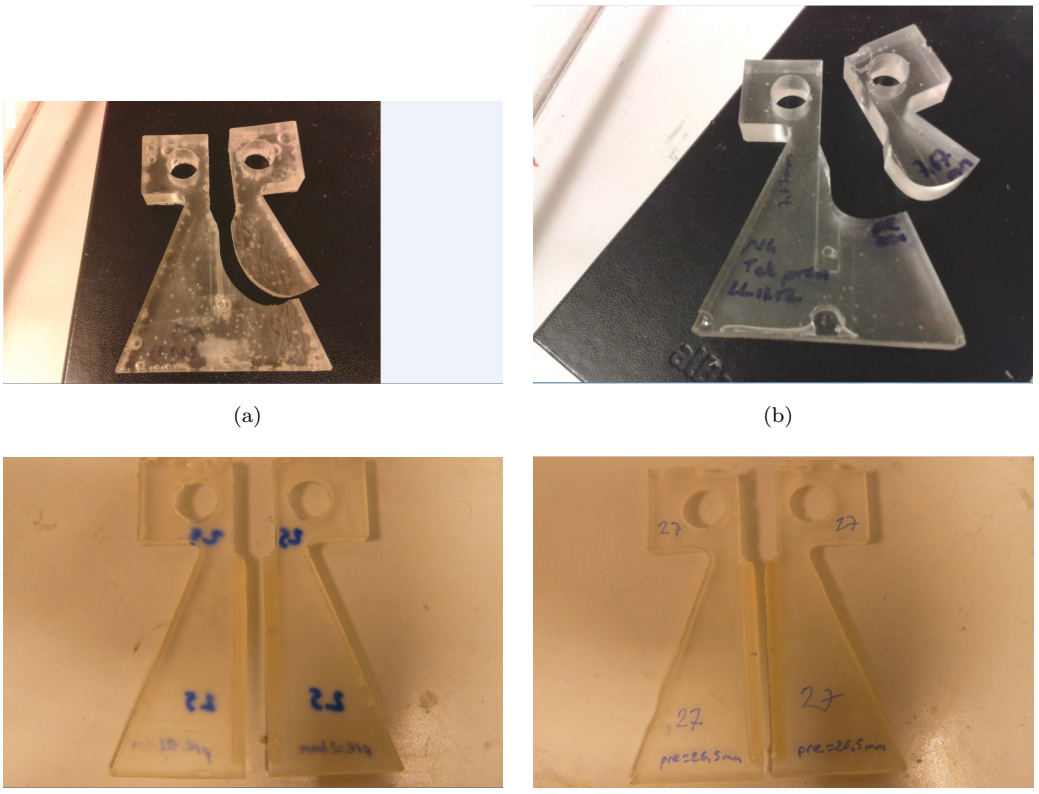

(a) (b)

(c) (d)

FIGURE 5.1: (a),(b) TDCB specimens without grooves (c),(d) samples with grooves.

Figure 5.2(b) indicates the formation of PhCl-loaded microcapsules.

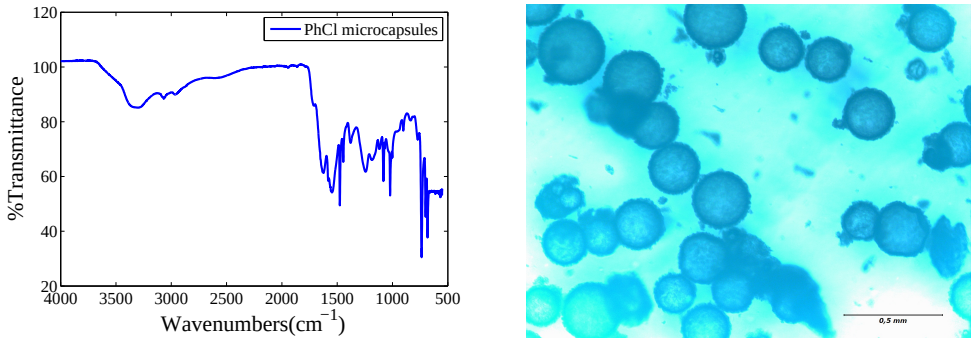

(a) (b)

FIGURE 5.2: (a)Mid-IR spectra of PhCl-loaded microcapsules, and (b) An optic image of PhCl-loaded microcapsules

A series of control fracture samples were fabricated and tested to investigate the intrinsic self healing concept for epoxy based host materials as well as the effect

of PhCl which is added to the healing agent for decreasing its viscosity. Towards this end, four different types of experiments have been performed. Of these, two of the control experiments have been devoted to the investigation of the PhCl on the self healing process. In the first type, TDCB samples with PhCl-loaded capsules were prepared and tested mechanically through using mode-I fracture test. In the second control experiment, the neat epoxy-TDCB specimens were prepared and fractured. Thereafter, 20 μl of PhCl was applied to the crack surfaces of the specimen before the heat treatment process. Then crack surfaces of specimens for the first and the second control experiments were brought together and then the specimens were put into the oven for heat treatment for a day. After the heat treatment, it is noted that the fractured samples did not show any sign of adhesion between crack surfaces, implying that the PhCl does not influence the self healing process. In the third type, we have performed mode-I fracture test on TDCB specimens having only neat epoxy without encapsulated healing agent. The fractured surfaces of neat TDCB specimens are brought together and then put into an oven for the duration of 12-24 hours, and again it was observed that the cracked surfaces did not experience any healing since after the heat treatment there was no observable adhesion between the crack surfaces. In the fourth experiment, TDCB samples with epoxy-loaded microcapsules and without any catalyst containing microcapsules were prepared and tested mechanically through using mode-I fracture test. The same procedure as described above has been applied for self-healing, and this time, it has been noted that the healing solution has partially underwent polymerization due to the presence of excess amines in the host material and therefore healing the crack with moderate success.

Mechanical properties of epoxy resin containing 20% microcapsules were investigated by conducting the 3-point bending tests. Experiments have indicated that the incorporation of microcapsules into the epoxy matrix adversely affects the flexure behavior of the samples since in essence micron size microcapsules act as crack initiation points or defects hence decreasing the flexural performance of the host material. The presence of microcapsules in the host material has made the host material brittle since microcapsules-incorporated flexure test specimens have showed a more brittle like behavior whereas samples without any microcapsules have revealed relatively ductile behavior as can be seen in Figure 5.3.

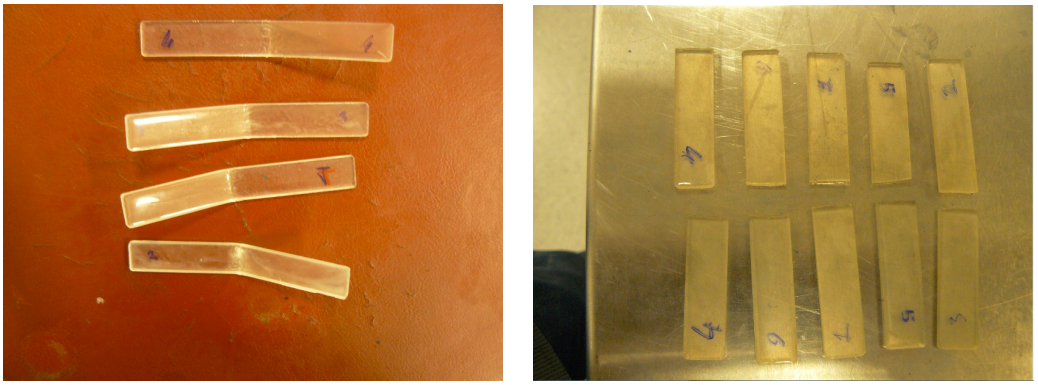

(a) (b)

FIGURE 5.3: (a)Neat compression specimen,(b) Compression specimen containing 20% microcapsules with a average diameter of 95.2 μm.

Although the scope of this work was specified as semi-intrinsic self-healing system, a total intrinsic self-healing material uses a latent functionality to trigger the healing mechanism instead of using a sequestered healing agent. A truly intrinsic self healing system can heal itself many times even though material is cracked from healed portion. On the other hand our concept do not provide a second healing cycle for the healed portion of material, because in the first healing cycle, healing agent is consumed to repair crack.

In the recent years two French companies Schlumberger and Arkema have developed and industrialized two different truly intrinsic self-healing material. The industrialized self healing product of Schlumberger is the FUTUR self healing cement. Schlumberger claims that their product FUTUR self-healing cement can be utilized to protect the integrity of a cementing casing of well. Arkema also announced that their truly intrinsic self-healing elastomer can be utilized in many applications such as conveyor belts, sealing joints, impact protection, insulation and shockabsorbing layers, industrial gloves, anti-corrosion coatings for metal, and formulation additives for adhesives, bitumen, organic binders, paints, varnishes, pastes and sealants. This truly intrinsic self healing system also repair itself many times by putting back the fracture surfaces together and applying a small pressure without any heat treatment.

Chapter 6

Conclusion

This work has initiated an interdisciplinary research in the field of self healed smart materials, which includes the production of microcapsules containing liquid healing agent and their characterization through using several techniques, the incorporation of the microcapsules into the base material, and finally mechanical characterization of microcapsules-containing base material by using TDCB specimen. The liquid-filled microcapsules-epoxy composite have showed poor healing efficiency due to the unavailability of the sufficient amount of un-reacted catalyst agent in the vicinity of the crack plane. The result of this work indicates that the intrinsic self-healing approach does not provide the required self-healing efficiency and to be able to achieve high self-healing efficiency, it is compulsory to have excess catalyst in the crack plane so that the released polymer healing liquid can be polymerized. This can be achieved by preparing microcapsules containing the catalyst. Another significant contribution of this thesis work is the effort to design a mechanical testing methodology to evaluate the self healing functionality of the studied material system. Towards this end, we have adopted the geometry of TDCB specimen utilized in literature to be able perform reliable Mode-I crack opening test

Although a moderate healing efficiency was recorded in this work, this study also showed that microcapsules can contribute both positively and negatively to mechanical behaviours of host material, meaning that even though the addition of microcapsules into epoxy based thermosetting materials increases the mode-I fracture toughness value of the self healing specimen, it severely decreases its flexural strength.

6.1 Future Direction

To eliminate the main drawback of this study, the first work to be done in the future should be the production of microcapsules containing hardener or the incorporation of the second catalyst phase to initiate the further polymerization of the healing solution. Moreover, in literature, there are a few immature studies on the encapsulation of hardener of epoxy, which indicates that different encapsulation methods and different encapsulation materials should also be attempted to encapsulate the poly-amine catalyst.

A new testing method to evaluate the self healing functionality should be investigated since when the diameter of microcapsules decreases, the evaluation of the self healing with TDCB specimen becomes rather impractical and unreliable. For example, the evaluation of the self healing with nano size capsules and liquid- filled fibers might be impossible, since nano-size fluid storage system might not fill the crack plane completely. If the crack plane is not filled completely, the adhesion between the failed TDCB beam will not be realized and $K_{IChealed}$ might not be obtained from the second test.

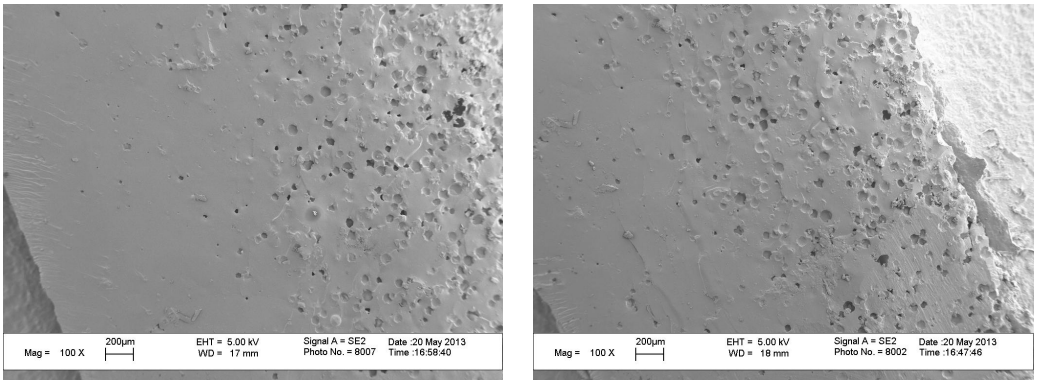

(a) (b)

FIGURE 6.1: Microcapsules tend to settle down in TDCB sample

The other important future work should investigate the density of microcapsules. Because when microcapsules are incorporated into the host material, if the density of microcapsules is higher than the base material, they tend to settle down. This precipitation harshly affects the self healing test of the TDCB specimen. If microcapsules are not distributed perfectly inside the base material, then precipitation occurs as shown in Figure 6.1.

A detailed mechanical behavior of microcapsule-incorporated epoxy resin must be examined as a future study. For example, tensile or compression properties of self healing specimen should be examined as a function of mean capsule diameter.

Appendix A

Appendix

In the early days of this work several attempts were done to characterize microcapsules by using Raman spectroscopy(Renishaw invia Raman Microscope). The raman results of the C1 microcapsule batch is presented in Figure A.1

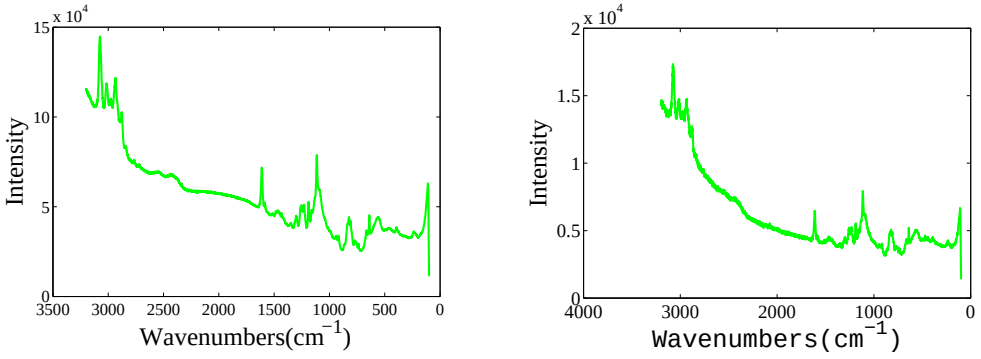

(a) (b)

FIGURE A.1: (a)Raman spectroscopy of C1 microcapsule batch

Bibliography

[1] Mary M. Caruso, Douglas A. Davis, Qilong Shen, Susan A. Odom, Nancy R. Sottos, Scott R. White, and Jeffrey S. Moore. Mechanically-induced chemical changes in polymeric materials. *CHEMCAL REVIEWS*, 109(11):5755–5798, 2009. doi: 10.1021/cr9001353. PMID: 19827748.

[2] EN Brown, SR White, and NR Sottos. Retardation and repair of fatigue cracks in a microcapsule toughened epoxy composite - part 1: Manual infiltration. *COMPOSITES SCIENCE AND TECHNOLOGY*, 65(15-16, SI): 2466–2473, DEC 2005.

[3] B. J. Blaiszik, S. L. B. Kramer, S. C. Olugebefola, J. S. Moore, N. R. Sottos, and S. R. White. Self-Healing Polymers and Composites. In Clarke, DR and Ruhle, M and Zok, F, editor, *ANNUAL REVIEW OF MATERIALS RESEARCH, VOL 40*, volume 40 of *Annual Review of Materials Research*, pages 179–211. 2010.

[4] Talha Boz. Structural health monitoring of composite materials with fbg sensors: Damage detection and remaining useful life prediction. Msc thesis, Sabanci University, September 2012.

[5] YH Kim and RP Wool. A Theory of Healing at a Polymer- Polymer Interface. *MACROMOLECULES*, 16(7):1115–1120, 1983.

[6] P.G. De Gennes. The formation of polymer/polymer junctions. In J.M. Georges, editor, *Microscopic Aspects of Adhesion and Lubrication Proceedings of the 34th International Meeting of the Socit de Chimie Physique*, volume 7 of *Tribology Series*, pages 355 – 367. Elsevier, 1981.

[7] K Jud, HH Kausch, and JG Williams. Fracture-Mechanics Studies of Crack Healing and Welding of Polymers. *JOURNAL OF MATERIALS SCIENCE*, 16(1):204–210, 1981.

[8] S Prager and M Tirrell. The Healing-Process at Polymer-Polymer Interfaces. *JOURNAL OF CHEMICAL PHYSICS*, 75(10):5194–5198, 1981.

[9] C Dry. Procedures developed for self-repair of polymer matrix composite materials. *COMPOSITE STRUCTURES*, 35(3):263–269, JUL 1996.

[10] C Dry and W McMillan. Three-part methylmethacrylate adhesive system as an internal delivery system for smart responsive concrete. *SMART MATERIALS & STRUCTURES*, 5(3):297–300, JUN 1996.

[11] M Motuku, UK Vaidya, and GM Janowski. Parametric studies on self-repairing approaches for resin infused composites subjected to low velocity impact. *SMART MATERIALS & STRUCTURES*, 8(5):623–638, OCT 1999.

[12] SM Bleay, CB Loader, VJ Hawyes, L Humberstone, and PT Curtis. A smart repair system for polymer matrix composites. *COMPOSITES PART A-APPLIED SCIENCE AND MANUFACTURING*, 32(12):1767–1776, 2001.

[13] MR Kessler and SR White. Self-activated healing of delamination damage in woven composites. *COMPOSITES PART A-APPLIED SCIENCE AND MANUFACTURING*, 32(5):683–699, 2001.

[14] SR White, NR Sottos, PH Geubelle, JS Moore, MR Kessler, SR Sriram, EN Brown, and S Viswanathan. Autonomic healing of polymer composites. *NATURE*, 409(6822):794–797, FEB 15 2001.

[15] Richard P. Wool. Polymer science: A material fix. *NATURE*, 409(6822): 773–774, 2001.

[16] EN Brown, MR Kessler, NR Sottos, and SR White. In situ poly(urea-formaldehyde) microencapsulation of dicyclopentadiene. *JOURNAL OF MICROENCAPSULATION*, 20(6):719–730, NOV-DEC 2003.

[17] JD Rule, EN Brown, NR Sottos, SR White, and JS Moore. Wax-protected catalyst microspheres for efficient self-healing materials. *ADVANCED MATERIALS*, 17(2):205+, JAN 31 2005.

[18] M. W. Keller and N. R. Sottos. Mechanical properties of microcapsules used in a self-healing polymer. *EXPERIMENTAL MECHANICS*, 46(6):725–733, DEC 2006.

[19] B. J. Blaiszik, N. R. Sottos, and S. R. White. Nanocapsules for self-healing materials. *COMPOSITES SCIENCE AND TECHNOLOGY*, 68(3-4):978–986, MAR 2008.

[20] MR Kessler and SR White. Cure kinetics of the ring-opening metathesis polymerization of dicyclopentadiene. *JOURNAL OF POLYMER SCIENCE PART A-POLYMER CHEMISTRY*, 40(14):2373–2383, JUL 15 2002.

[21] Timothy C. Mauldin, Joseph D. Rule, Nancy R. Sottos, Scott R. White, and Jeffrey S. Moore. Self-healing kinetics and the stereoisomers of dicyclopentadiene. *JOURNAL OF THE ROYAL SOCIETY INTERFACE*, 4(13):389–393, APR 22 2007.

[22] SH Cho, HM Andersson, SR White, NR Sottos, and PV Braun. Polydimethylsiloxane-based self-healing materials. *ADVANCED MATERIALS*, 18(8):997+, APR 18 2006.

[23] Soo Hyoun Cho, Scott R. White, and Paul V. Braun. Self-Healing Polymer Coatings. *ADVANCED MATERIALS*, 21(6):645+, FEB 9 2009.

[24] Jason M. Kamphaus, Joseph D. Rule, Jeffrey S. Moore, Nancy R. Sottos, and Scott R. White. A new self-healing epoxy with tungsten (VI) chloride catalyst. *JOURNAL OF THE ROYAL SOCIETY INTERFACE*, 5(18):95–103, JAN 6 2008.

[25] Steven D. Mookhoek, Benjamin J. Blaiszik, Hartmut R. Fischer, Nancy R. Sottos, Scott R. White, and Sybrand van der Zwaag. Peripherally decorated binary microcapsules containing two liquids. *JOURNAL OF MATERIALS CHEMISTRY*, 18(44):5390–5394, 2008.

[26] Joseph D. Rule, Nancy R. Sottos, and Scott R. White. Effect of microcapsule size on the performance of self-healing polymers. *POLYMER*, 48(12):3520–3529, JUN 4 2007.

[27] Eva L. Kirkby, Joseph D. Rule, Veronique. J. Michaud, Nancy R. Sottos, Scott R. White, and Jan-Anders E. Manson. Embedded shape-memory alloy wires for improved performance of self-healing polymers. *ADVANCED FUNCTIONAL MATERIALS*, 18(15):2253–2260, AUG 11 2008.

[28] E. L. Kirkby, V. J. Michaud, J. A. E. Manson, N. R. Sottos, and S. R. White. Performance of self-healing epoxy with microencapsulated healing agent and shape memory alloy wires. *POLYMER*, 50(23):5533–5538, NOV 3 2009.

[29] Henghua Jin, Gina M. Miller, Nancy R. Sottos, and Scott R. White. Fracture and fatigue response of a self-healing epoxy adhesive. *POLYMER*, 52(7): 1628–1634, MAR 23 2011.

[30] David A. McIlroy, Benjamin J. Blaiszik, Mary M. Caruso, Scott R. White, Jeffrey S. Moore, and Nancy R. Sottos. Microencapsulation of a Reactive Liquid-Phase Amine for Self-Healing Epoxy Composites. *MACROMOLECULES*, 43 (4):1855–1859, FEB 23 2010.

[31] Henghua Jin, Chris L. Mangun, Dylan S. Stradley, Jeffrey S. Moore, Nancy R. Sottos, and Scott R. White. Self-healing thermoset using encapsulated epoxy-amine healing chemistry. *POLYMER*, 53(2):581–587, JAN 24 2012.

[32] Jinglei Yang, Michael W. Keller, Jeffery S. Moore, Scott R. White, and Nancy R. Sottos. Microencapsulation of Isocyanates for Self-Healing Polymers. *MACROMOLECULES*, 41(24):9650–9655, DEC 23 2008.

[33] E.N. Brown, SR White, and NR Sottos. Retardation and repair of fatigue cracks in a microcapsule toughened epoxy composite - Part II: In situ self-healing. *COMPOSITES SCIENCE AND TECHNOLOGY*, 65(15-16, SI): 2474–2480, DEC 2005.

[34] E. N. Brown, S. R. White, and N. R. Sottos. Fatigue crack propagation in microcapsule-toughened epoxy. *JOURNAL OF MATERIALS SCIENCE*, 41 (19):6266–6273, OCT 2006.

[35] A. S. Jones, J. D. Rule, J. S. Moore, N. R. Sottos, and S. R. White. Life extension of self-healing polymers with rapidly growing fatigue cracks. *JOURNAL OF THE ROYAL SOCIETY INTERFACE*, 4(13):395–403, APR 22 2007.

[36] M. W. Keller, S. R. White, and N. R. Sottos. Torsion fatigue response of self-healing poly(dimethylsiloxane) elastomers. *POLYMER*, 49(13-14):3136–3145, JUN 23 2008.

[37] Dcpd- material safety data sheet, nova chemicals. .

[38] National toxicology program (10 june 2011). "12th report on carcinogens". national toxicology program. retrieved 2011-06-11, .

[39] B. J. Blaiszik, M. M. Caruso, D. A. McIlroy, J. S. Moore, S. R. White, and N. R. Sottos. Microcapsules filled with reactive solutions for self-healing materials. *POLYMER*, 50(4):990–997, FEB 9 2009.

[40] P. P. Grad and R. J. Dunn. Determination of mole ratio of urea to formaldehyde. *Analytical Chemistry*, 25(8):1211–1214, 1953.

[41] G. I. Taylor. The viscosity of a fluid containing small drops of another fluid. *Proceedings of the Royal Society of London. Series A*, 138(834):41–48, 1932.

[42] Li Yuan, Guo-Zheng Liang, Jian-Qiang Xie, Jing Guo, and Lan Li. Thermal stability of microencapsulated epoxy resins with poly(urea-formaldehyde). *POLYMER DEGRADATION AND STABILITY*, 91(10):2300–2306, OCT 2006.

[43] Cabanelas J.C. Gonzales M.G. and Baselga J. Applications of ftir on epoxy resin- idenfication, monitoring the curing process, phase separation and water uptake. *InTech*, 2012.

[44] L.A. Harrah, M.T. Ryan, and G. Tamborski. Infrared spectra of phenyl derivatives of group ivb, vb and {VIIb} elements. *Spectrochimica Acta*, 18 (1):21 – 37, 1962.

[45] J.G.Williams D.R. Moore, A. Pavan. *Fracture Mechanics Testing Methods for Polymers Adhesives and Composites*. ESIS Publication 28. ELSEVIER, 2001.

[46] W Beres, AK Koul, and R Thamburaj. A tapered double-cantilever-beam specimen designed for constant-K testing at elevated temperatures. *JOURNAL OF TESTING AND EVALUATION*, 25(6):536–542, NOV 1997.

[47] EN Brown, NR Sottos, and SR White. Fracture testing of a self-healing polymer composite. *EXPERIMENTAL MECHANICS*, 42(4):372–379, DEC 2002.

[48] E. N. Brown. Use of the tapered double-cantilever beam geometry for fracture toughness measurements and its application to the quantification of self-healing. *JOURNAL OF STRAIN ANALYSIS FOR ENGINEERING DESIGN*, 46(3):167–186, APR 2011.

[49] Hunstman Advanced Materials. Automotive parts manufacturing selector guide, 2006, Switzerland.

[50] EN Brown, SR White, and NR Sottos. Microcapsule induced toughening in a self-healing polymer composite. *JOURNAL OF MATERIALS SCIENCE*, 39(5):1703–1710, MAR 1 2004.

[51] Standard test methods for flexural properties of unreinforced and reinforced plastics and electrical insulating materials, astm d 790-03. .